Faculty of Science
University of South Bohemia

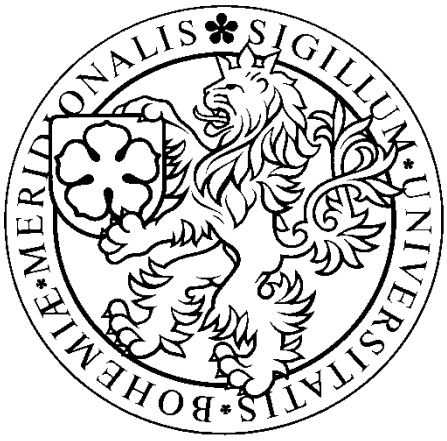

Identification of interacting partners of Discs overgrown *in vivo*

Master thesis

Bc. Petra Houfková

Supervised by: Mgr. Lukáš Trantírek, Ph.D.

České Budějovice, 2009

Houfková, P., 2009: Identification of interacting partners of Discs overgrown *in vivo.* Mgr. Thesis, 59 pp. Faculty of Science, University of South Bohemia, České Budějovice, Czech Republic

Annotation

The mutated forms of the *Discs overgrown* gene causes overproliferation of imaginal discs of *Drosophila melanogaster*. Somatic mutations in its human counterpart, casein kinase I epsilon, were strongly associated with human breast cancer. Using the advantage of a high conservancy between fly's *dco* and human *casein kinase I epsilon* genes we have chosen *D. melanogaster* as a model organism to provide a list of probable Dco interaction partners via tandem affinity purification and mass spectrometry analysis. However, these proteins need to be independently verified as true Dco interaction partners.

This project was supported by Grant Agency of the Czech Republic (301/07/0814) and by Student Grant Agency of the Faculty of Science, University of South Bohemia (SGA2007/007 and SGA2008/006).

Prohlašuji, že jsem uvedenou práci vypracovala samostatně, pouze s použitím uvedené literatury.

Prohlašuji, že v souladu s § 47b zákona č.111/1998 Sb. v platném znění souhlasím se zveřejněním své diplomové práce, a to v nezkrácené podobě elektronickou cestou a na veřejně přístupné části databáze STAG provozované Jihočeskou univerzitou v Českých Budějovicích na jejích internetových stránkách.

V Českých Budějovicích, 15. 1. 2009 .....

Acknowledgements

I would like to thank to my supervisor Lukáš Trantírek as well as to Tomáš Doležal for the opportunity to work in their labs, for their help and patience.

I owe special thanks to Peter Koník for running the MS analyses, for teaching me the ´MS operation´ and also for ´giving hope and keeping faith´.

My thanks belong to Dr. Alexey Veraksa (University of Massachusetts, Boston), who kindly provided us the vectror pUAST-CTAP.

I would like to thank to all members - friends, respectively - of Laboratory of Structural Biology and Laboratory of Developmental Genetics for creating the best working space within two gallaxies.

I would like to thanks to my family and all my friends (especially to P. and to those mentioned previously again) for their neverending support and to JM for standing the darkness.

Contents

1. Introduction

1.1. Casein Kinase I epsilon/ Discs Overgrown and Breast Cancer

With a million new cases in the world each year, breast cancer is the most common malignancy in women. Of every 1000 women aged 50, two will recently have had breast cancer diagnosed and about 15 will have had a diagnosis made before the age of 50 (McPherson et al, 2000). In 2006 in Europe, breast cancer was by far the most common form of cancer diagnosed in European women, accounting 429 900 cases (28.9% of total). With the continuous increase of early diagnosed cases, breast cancer has become the most common form of cancer diagnosed in Europe, and it has been the third major cause of cancer death (131 900, 7.8% of total); (Ferlay et al., 2007).

About 10% of breast cancers may occur due to genetic predisposition (Emery et al., 2001). Breast cancer susceptibility is generally inherited as an autosomal dominant with limited penetrance. The best-known genes associated with breast cancer, *BRCA1* and *BRCA2*, have been identified to account for a substantial proportion of very high risk families – i.e. those with four or more breast cancers among close relatives. Both genes are very large and mutations can occur at almost any position, so that molecular screening to detect mutation for the first time in an affected individual or family is technically demanding. Certain mutations occur at high frequency in defined populations (McPherson et al., 2000). However, only about 20% of familial cases are connected with inherited mutations in *BRCA1* and *BRCA2* genes. Inherited mutations in two other genes, *p53* and *PTEN*, are associated with familial syndromes (Li-Fraumeni and Cowden's, respectively) that include a high risk of breast cancer, but both are rare (McPherson et al., 2000).

Large portion of the familial cases and even bigger portion of somatic occurrence of breast cancer are still waiting to be explained at the molecular/genetic level.

Remarkably high frequency of somatic mutations was found in *casein kinase I epsilon* (*CKIε*) in patients with breast cancer (Fuja et al., 2004). Mutations in *Drosophila melanogaster* homologue of human *CKIε, Discs overgrown* gene (*dco),* causes analogous phenotype to human breast cancer: mutant larvae (*dco3*) fail to arrest growth of imaginal discs when they reach their normal size and the discs grow continuously to several times the wild-type final size (Jursnich et al., 1990). The comparison of the CKIε/Dco protein sequence with marked mutations is shown in the Fig. 1.1.

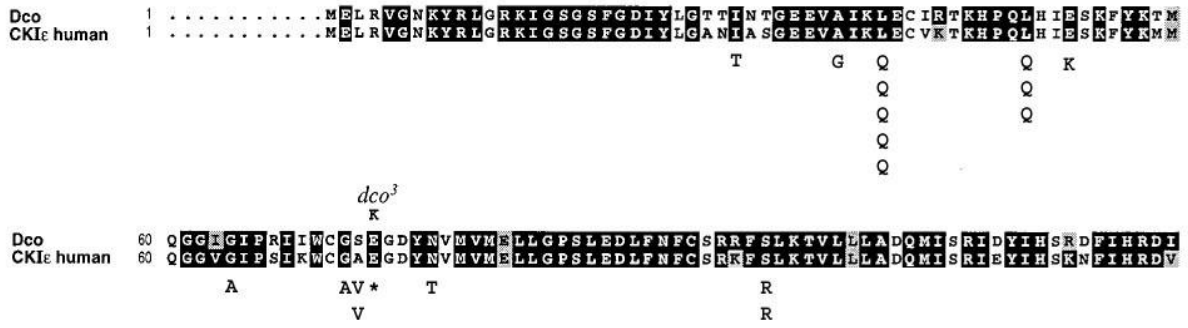

Fig. 1.1: Comparison of the protein sequence of amino-terminal part of the Dco of *D. melanogaster* and human CKIε. Mutation causing the over-growing phenotype in *dco3* larvae of *D. melanogaster* is shown above the sequence and 19 somatic mutations found in the breast cancer tissue are marked below (Fuja et al., 2004).

1.2. Casein Kinase I (CKI) Family

The CKI is a family of monomeric multi-functional serine (Ser)/threonine (Thr) protein kinases (in human approx. 37—51 kDa). It is found in eukaryotic organisms from yeast to human and is ubiquitously expressed in different cell types (Gross and Anderson, 1998; Vielhaber and Virshup, 2001). Seven family members (referred to as isoforms, but encoded by distinct genes) have been identified in mammals: α, β, γ 1-3, δ, and ε.

The family members have the highest homology in their kinase domains (53% – 98% identical) and differ mainly in length and primary structure of the regulatory C-terminal non-catalytic domain, but also within their N-termini.

CKIα and CKIδ are 76% identical outside their kinase domains, the CKIγ isoforms are ~50% identical in their C-terminal tails, and the long C-terminal extensions of CKIδ and CKIε have ~53% identity.

The long C-terminal extensions of CKIδ and CKIε are autophosphorylated, and this phosphorylation *in vitro* markedly inhibits the activity of the kinase domain (Gietzen and Virshup, 1999). Although they are able to autophosphorylate, they are in many cases maintained in the dephosphorylated state by phosphatases *in vivo* (Rivers et al., 1998).

Phosphorylation motifs for CKI on various functional acidic proteins have been characterized. The canonical phosphoacceptor sites are specified by a $(D/E)_x$-X-X-S/T and p(T/S)$(X)_{2-3}$S*/T* consensus, where p(T/S) indicates a phosphoserine or phosphothreonine, X any other amino acid, and S* the target serine or threonine that will receive the phosphoryl group from ATP. The phosphorylated amino acid, however, can be replaced by an aspartic

acid at position *n* - 3 (Songyang et al., 1996) or even more efficiently by a stretch of acidic amino acids (Pulgar et al., 1999).

In addition, a non-canonical motif can be depicted as $S^*LS(X)_{n\text{-}2\text{-}5}(D/E)_{2\text{-}5}$, in which the serine targeted for phosphorylation is the first of a SLS triplet followed by a cluster of acidic amino acids situated two to five residues downstream (Marin et al., 2002). A novel non-canonical motif that fulfills criteria for casein kinase II targeting, was proven as CKIδ target (Ferrarese et al, 2007). This S1510 residue of adenomatous polyposis coli (APC) is one of those whose phosphorylation is critical for association with β-catenin (Ha et al., 2004). CKI phosphorylation can also occur upon binding to the FXXXF docking motif (Marin et al., 2003; Okamura et al., 2004). Another novel phosphorylation motif (K/R-X-K/R-X-X-S/T) for CKI (δ,ε and γ) was identified by Kawakami et al., 2008 in several sulfatide and cholesterol-3-sulfate binding proteins (SCS-BPs). Binding of SCS to the proteins causes their conformational changes, which presumably facilitates their high phosphorylation by CKI (Okano et al., 2004). The mentioned motif is common consensus phosphorylation site of members of the Rho family and Kawakami et al., 2008 showed that in the presence of SCS, CKIγ RhoA phosphorylation was highly stimulated.

The CKI family is involved in a lot of diverse and important cellular functions (for review, see Knippschild et al., 2005a), such as regulation of membrane transport, vesicular trafficking, cell proliferation, apoptosis, DNA repair, nuclear localization, activity of various transmembrane receptors and plays an essential role in regulating several critical processes, such as circadian rhythm, embryogenesis and morphogenesis via Wnt signaling in various species.

Mutations and deregulation of CKI expression and activity has been linked to various diseases including neurodegenerative disorders such as Alzheimer's and Parkinson's disease, sleeping disorders and proliferative diseases such as cancer.

It was shown that CKI isoforms differentially associate with neurofibrillary and granulovacuolar degeneration lesions, whose appearance characterizes individuals affected with Alzheimer's disease (Ghoshal et al., 1999; Kannanayakal et al., 2006). Moreover, overexpression of constitutively active CKIε leads to an increase of the neurotoxic peptide amyloid-β peptide production (Flajolet et al., 2007).

Importantly, CKI is involved in various signal transduction pathways that are linked to cancer development (for review see, Knippschild et al., 2005b), as follows.

CKI is involved in Wingless (Wnt) and Hedgehog (Hg) signaling (Price, 2006) that share many similar features and both have been implicated in the initiation and maintenance of many types of tumors. It is known that some regulatory genes of Wnt pathway are mutated in primary human cancers (for review see, Polakis, 2007). In addittion, Umar et al., 2007 suggested that CKIε activation *in vivo* might be a biologically relevant mechanism to modulate β-catenin stability in hyperproliferating epithelia. Moreover, results of Sotgia et al., 2005 suggest that loss of calveolin-1, which causes hyperactivation of Wnt/β-catenin signaling cascade, induces the accumulation of mammary stem cells. This event may be an initiating factor during mammary tumorigenesis.

Furthermore, Modak and Bryant, 2008 suggested that CKIε is a positive regulator of the Akt pathway that also paticipates in cancer developement.

It is known that tumor supressor protein p53 is phosphorylated by CKI α, δ and ε upon cellular stress, which influences its transcriptional activity. Phosphorylation of threonine 18 by CK1δ/ε is believed to weaken the interaction of p53 with its inhibitory counterpart, oncoprotein Mdm2, thereby stabilizing and activating p53 function (Sakaguchi et al., 2000; Dumaz et al., 1999).

1.3. Discs overgrown

Drosophila Discs overgrown (Dco) is a 440 amino acids long phosphorylation enzyme and its three hundred N-terminal amino acids have a high level of sequence identity with the catalytic domain of members of the CKI family. The most closely related isoforms is human CKIε, with 86% sequence identity and 92% similarity through the kinase domain.

Zilian et al., 1999 identifitified *dco* gene when analyzing mutants showing excess cell proliferation in imaginal discs. Mutations of *dco* gene exhibit broad spectrum of phenotype effects ranging from the absence of discs to their over-proliferation. Hyperplastic growth of imaginal discs that exihibit defects in gap-junctional communication (Jursnich et al., 1990) was proven to be a *dco* phenotype for at least one allele by Zilian et al., 1999 (Fig. 1.2).

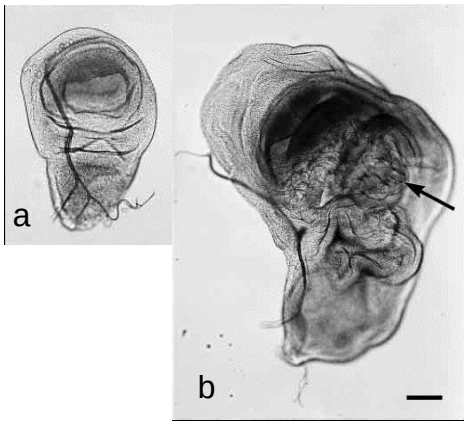

Fig. 1.2: Overgrowth of imaginal wing discs in a *dco* mutant. Scale bar, 100 μm.
(a) Wild-type wing disc, 5 days after oviposition. (b) *dco3/Df(3R)PH3*, heteroallelic combination of *dco3* allele exhibiting the mutation shown in Fig. 1.1 and of *dco* deficiency, 8 days after oviposition. Intensively overgrown disc with a central area (arrow) showing highly folded epithelial layers (taken from Zilian et al., 1999).

Zilian et al., 1999 stated that *dco* is identical to the previously cloned *double-time* (*dbt*) gene (Kloss et al., 1998). Dco regulates the circadian phosphorylation of Period (Per), thus controlling Per subcellular localization and stability (Cyran et al., 2005). It is also required for Clock (Clk) phase-specific hyperphosphorylation enhancing its degradation (Kim and Edery, 2006). The present model of *Drosophila* circadian rhythm is reviewed by Hardin, 2005 or Bae and Edery, 2006. Dco-directed Per phosphorylation sites have been mapped by Kivimäe et al., 2008. Mutations in *dco* can shorten or lenghten the period of circadian behavioral rhythms in *Drosophila* and all of them produce lowered kinase activity. For example, an expression of *dco* exhibiting K38R mutation, which specifically eliminates kinase activity, damped the oscillation of Per *in vivo* and caused arrhythmicity and very long circadian periods (Muskus et al., 2007). Mutations of its human ortholog has been associated with certain forms of a heritable sleep disorder, such as familial advanced sleep phase syndrome (FASPS) and delayed sleep phase syndrome (DSPS). Known *CKIδ/ε* gene variations are *CKIδ* T44A mutation found in FASPS (Xu et al., 2005), a *CKIε* S408N variation relevant to DSPS (Takano et al. 2004), and a *CKIε* R178C mutation in a hamster tau mutant (Lowrey et al., 2000).

Mutations in the phosphorylation sites of the CKIε substrates are also connected with disorders. For example the V647G variation of the *Per3* gene is linked to DSPS (Ebisawa, 2001).

Dco is involved in various pathways and phosphorylates numerous proteins. In fly cell culture and the wing imaginal discs, dco has been shown to be required for Wingless (Wg) signaling.

Cong et al., 2004 demonstrated that Dco positively regulates Wg pathway through Dishevelled and negatively regulates the planar cell polarity pathway. They suggest that Dco functions as a molecular switch to direct Dishevelled from the planar cell polarity pathway (PCP) to the canonical Wg pathway.

Klein et al., 2006 demonstrated *in vivo* in *Drosophila* through a series of loss-of-function and coexpression assays that Dco/CKIε acts positively for signaling in both pathways, rather than as a switch.

These results were confirmed by Strutt et al., 2006. Examining hypomorphic mutations of the *Drosophila dco*, they showed that it is an essential component of the noncanonical/PCP pathway. Moreover genetic interactions indicated that *dco* acts positively in planar polarity signaling. Further, Zhang et al., 2006 proved that *dco* had also a negative role in addition to its predominantly positive role in the Wg pathway.

On the other hand, Guan et al., 2007 found that cells homozygous for a null *dco* allele have normal Wg signaling in the developing wing. Their data support a model where Dco coordinates tissue size by stimulating cell division/growth and blocking apoptosis via activation of caspase inhibitor DIAP1 expression.

Jia et al., 2005 explored the role of Dco/CKIe in the Hh pathway in developing *Drosophila* wings using genetic mutations, dominant-negative kinase, and RNA interference (RNAi). They proved that Dco participates in processing of Hh final actor Cubitus Interruptus (Ci).

Results of Cho et al., 2006 imply that Dco is also involved in the Hippo signaling. The core components of the Hippo pathway are known to be conserved between *Drosophila* and mammals (for review, see Zhao et al., 2008). Moreover, dysregulation of the Hippo pathway contributes to the loss of contact inhibition observed in cancer cells. Therefore, the Hippo pathway connects the regulation of organ size and tumorigenesis (Zhao et al., 2008).

1.4. *Drosophila melanogaster* as a Model Organism

Drosophila has been used as a model organism to identify genes involved in the regulation of cell proliferation and tumorigenesis. High level of gene and pathway conservation, similarity of cellular processes and emerging evidence of functional conservation of tumor suppressors between *Drosophila* and mammals, validate that studies of

tumorigenesis in flies can directly contribute to the understanding of human cancer (Potter et al., 2000). Since the fly genome has been sequenced, functions of numerous proteins have been revealed, multiple genetics tools have been developed, and phenotypes of gene/protein manipulation can be easily observed, it is the proper model organism to study connections inside and between the signaling pathways.

1.4.1. Balancer Chromosomes

An advantage can be taken of using the *Drosophila* balancer chromosomes. They contain multiple inversions and in combination with a wild-type chromosome, there are no viable crossover products. Thus it is possible to keep stable lines (also with lethal mutations). Balancer chromosomes are usually marked with a dominant morphological mutation (for example *Curly*, *Stubble*, *Beaded-Serrate*, *Tubby*), which allows tracking of the segregation of the entire balancer or its normal homologue by following the presence or absence of the marker. They can also carry a recessive genetic marker causing lethality in homozygous state (Griffiths at al., 1999; Dahmann, 2008).

1.4.2. *D. melanogaster* P-elements

P-element-mediated gene transfer is another useful genetic tool that results in stable integration of exogenous DNA into the germline of *D. melanogaster*. P-elements are transposable elements capable of random genome incorporation. They are classified as autonomous or nonautonomous, depending on their capability to transpose. They vary in size, but there is always a 31-bp perfect inverted repeat (IR) at their ends and 11 bp inverted subterminal repeats occur as the major *cis*-acting target sequences for excision by transposase. A full-sized P-element carries a *transposase* gene that is responsible for its mobilization. In order to use P-elements as a genetic tool, IRs have been integrated into plasmid vectors separately from the *transposase* gene. The gene of our interest can be inserted between the IRs, and the mobilization and genome incorporation is caused by transposase transcribed from a helper plasmid (Griffiths at al., 1999; Dahmann**,** 2008).

1.4.3. Gal4/ UAS System

Gal4 encodes a protein identified in the yeast *Saccharomyces cerevisiae* as a regulator of genes induced by galactose. Gal4 regulates the transcription of the divergently transcribed *GAL10* and *GAL1* genes by direct binding to four related 17 bp sites located between these loci. These sites define an Upstream Activating Sequences (UAS) element, analogous to an enhancer element defined in multicelluar eukaryotes, which is essential for the transcriptional activation of these Gal4-regulated genes (Duffy, 2002).

It was demonstrated that Gal4 expression was capable of stimulating transcription of a reporter gene under UAS control in *Drosophila* (Fischer et al., 1988) and a system for targeted gene expression in *Drosophila* was developed (Fig. 1.2).

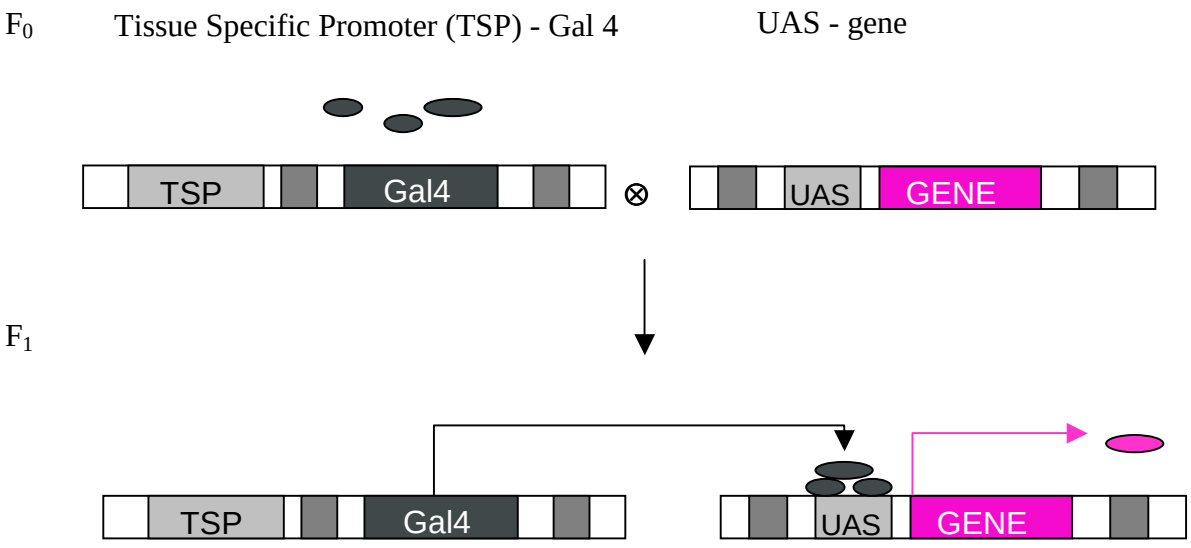

Fig. 1.2: Scheme of the Gal4/UAS system for *Drosophila* transgenic expression.
In F_0 generation, one transgenic line expresses GAL4 in a known temporal or spatial pattern and a second transgenic line, the responder, contains a UAS-dependent transgene. Their cross leads to the F_1 progeny that exhibit both *Gal4* driver under tissue specific promoter (TSP) and gene of our interest under the UAS. This results in the transcription of responder gene in tissue specific pattern.

1.5. Aims of the Thesis

Since the mutations of the CKIε protein could have an effect on breast cancer development, the more we know about the wild type CKIε/Dco interaction partners, the better target it becomes for the prediction of effective compounds affecting it in the clinical setting. Recently, an inhibitor of CKIε, IC261, showed cancer-selective growth inhibition in HT1080 cell culture (Yang and Stockwell, 2008).

High similarity of CKIε and Dco allows use of *D. melanogaster* as a model organism for investigation of the role of human CKIε in breast cancer. If we determine Dco/CKIε interactors, we will better distinguish its role in the process of tissue growth control and its connection among the signalling pathways. Such results could further serve for the comparison of wild type Dco/CKIε interactors with the interactors of Dco/CKIε affected by oncogenic mutations, including those given in Fig 1.1. Theoretically, mutations in the initial kinase (Dco/CKIε) need not be the only reason of the breast cancer development – mutations in the protein's target site (phosphorylation sites of the Dco/CKIε substrates) could be involved, as well. The mapping of the substrates of Dco/CKIε is therefore necessary for further conclusions.

In this thesis, we aimed at characterozation of the interaction partners of the Dco protein using *D. melanogaster* as a model organism. This aim is reachable via the tandem affinity purification (TAP) method. For this purpose, the coding region of the *dco* gene will be fused together with the C-terminal TAP (CTAP) tag, which serves as an anchor for purification of the Dco protein accompanied by its interactors. The coding region of the *dco* gene will be inserted into the pUAST-CTAP vector, which allows *Drosophila* embryo transformation and selective expression of the protein in specific tissues using UAS/Gal4 system. The TAP-tagged Dco protein will be purified under native conditions, associated partners will be characterized using mass spectrometry and given into connection with known facts about Dco/CKIε.

The strategy could be summarized as:

1. Preparation of transgenic *D. melanogaster* carrying TAP-tagged *dco.*

2. Expression of TAP-tagged Dco in imaginal discs of the late-third instar *D. melanogaster* larvae using UAS/Gal4 system.

3. Purification of TAP-tagged Dco protein from the crude *Drosophila* larvae extract under native conditions using the tandem affinity purification (TAP).

4. Identification of the associated partners of the Dco protein using mass spectrometry.

2. Material and Methods

2.1. Preparation of TAP-tag Construct

Entire coding region of the *dco* gene is situated in its fourth exon. Coding region of *dco* was cloned into the pUAST-CTAP vector (GenBank accession number for its complete sequence is AY727856), (Fig. 2.1) allowing *Drosophila* embryo transformation (contains P-element and the *mini white+* gene as a transformation marker), selective expression of the protein in specific tissues using UAS/Gal4 system and introducing a carboxy-terminal TAP (CTAP) tag with the coding region of the protein of interest.

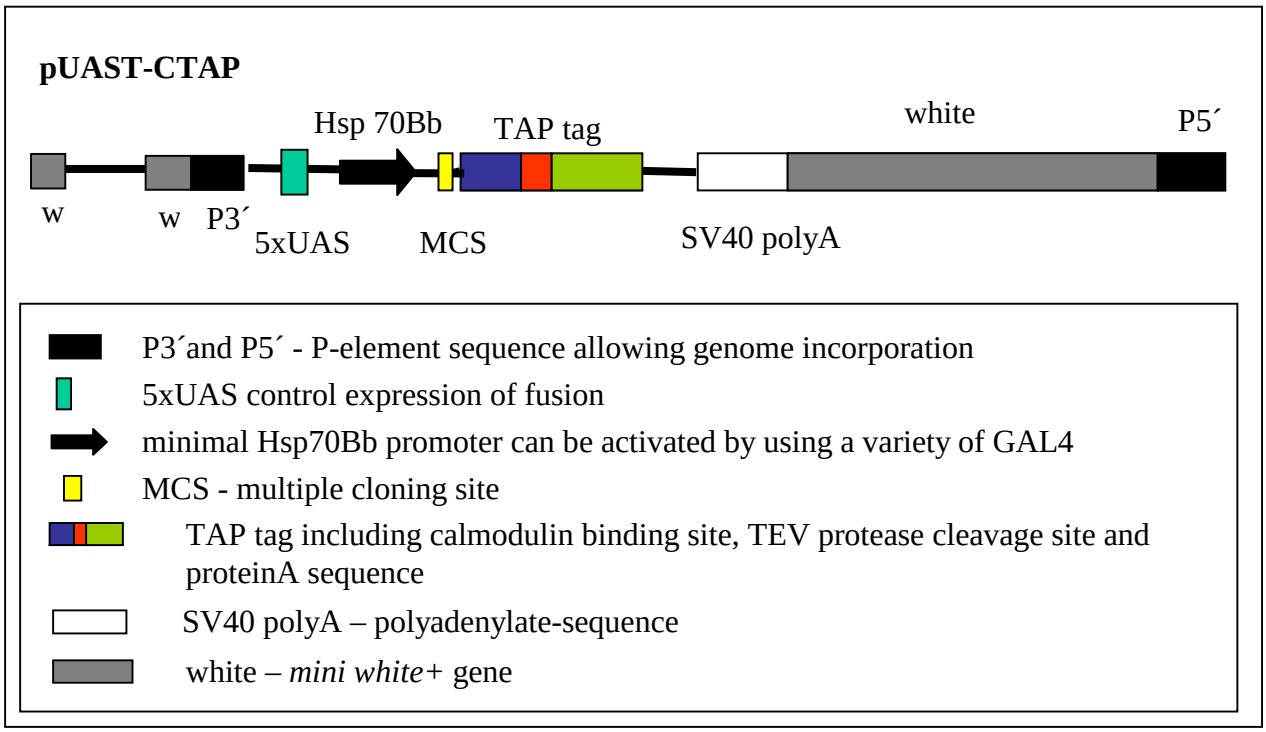

Fig. 2.1: Scheme of the pUAST-CTAP vector.

PCR primers were designed to amplify the coding region of the *dco* gene. The forward primer contained the *Xho I* site and the reverse the *Kpn I* site (Tab. 2.1).

Tab. 2.1: Primers used to amplify the *dco* gene.

Primer	Restriction site	Sequence 5´→3´
Forward	*Xho I*	CTCGAGATGGAGCTGCGCGTGGGTA
Reverse	*Kpn I*	GGTACCTTTGGCGTTCCCCACGCCA

The gene was amplified under the following conditions: denaturation 10 seconds at 98°C; followed by 30 cycles of 1 second denaturation at 98°C and 20 seconds annealing with elongation at 72°C; final extension was done at 72°C for 1 minute. For amplification, Phusion Flash High-Fidelity PCR Master Mix (Finnzymes) was used according to manufacturer´s instructions.

The PCR product of expected size (1322 bp) was gel purified (ZYMO RESEARCH) and A overhangs were added to the blunt PCR product. 10 µl of 10mM dATP, 10 µl 10x PCR Buffer, 5 µl DNA, 1 µl TaKaRa Taq DNA polymerase (5 units/µl) and distilled water up to 100 µl were incubated at 72°C for 2 hours.

This product was subcloned into the pGEM T-easy vector (Promega). The insert was cut out by *Xho I* and *Kpn I* restriction enzymes (both NEW ENGLAND BioLabs) and cloned into the pUAST-CTAP vector cut with the same enzymes. CTAP tag was introduced in-frame with the coding region of the protein of interest.

Insert and CTAP tag region was checked by sequencing by Macrogen, Korea using primers listed in Tab. 2.2. SQ1 and SQ6 primers are complementary to the plasmid sequence, the rest to the *dco*/CTAP region.

Tab. 2.2: Primers used for sequenation.

Primer	Sequence 5´→3´
SQ1	CAATTCAAACAAGCAAAGTGAACACG
SQ2	CTCGAGATGGAGCTGCGCGTGGGTA
SQ3	CCTCGATTGTGGTGCTGTGC
SQ4	AAGTTGCGGAAGAGTTTG
SQ5	GGTTGGCTGCTGAGACGGCTATGA
SQ6	ATGGCATTTCTTCTGAGCAAAACAG

2.2. Fly Stock and Culture

For standard procedures, flies were raised at 25°C on a standard diet (120 g cornmeal, 15 g agar, 75 g sacharose, 60 g instant yeast in 1.5 L of water) supplemented with 25 mL of 10% methyparaben in ethanol.

The list of fly stocks used in this work is shown below in Tab. 2.3.

Tab. 2.3: Fly stocks used in this work.

Used genetic aberrations are summarized and explained in Lindsley and Zimm, 1992.

Stock code	Characterization	Notes
281	*yw; xa/CyO, MKRS*	Compound II + III chromosome with xa marker
arm	*arm > Gal4*	armadillo-Gal4, II chromosome
339	*arm > Gal4*	III chromosome
340	*arm > Gal4*	II chromosome
560	w^{1118}*; P{*$w^{+mW.hs}$*=GawB}C855a*	various tissues > Gal4, Gal4 expressed in larval optical lobe, wing disc, leg and eye disc peripodial membrane and fat body
565	*yw; P{* $w^{+mW.hs}$*=UAS-GFP}*	UAS-GFP, II chromosome
573	*yw*	X chromosome
604	*yw; xa/CyO Act>GFP; TM3 Act>GFP*	
606	*w; Sco/CyO; karel/TM6B*	
1012	*yw; FRT82 dco[le88]/TM6B Tb*	*dco* lethal phenotype
1015	*Df(3R)A177der22 ry[+]/TM6B Tb*	*dco* deficiency
1018	*act-Gal4/TM6B Hu Tb*	actine-Gal4, III chromosome
1063	*yw; letdelta76/yw FM6B*	X chromosome

2.3. Production of Transgenic Flies

2.3.1. DNA Preparation

The pUAST-CTAP construct and the helper P-element plasmid pπ25.7wc were purified using the Qiagen Plasmid Midi Preps Kit according to the manufacturer´s protocol.

3.5 µg of *dco*-CTAP pUAST construct was mixed with 1.5 µg of pπ25.7wc and precipitated by adding 1/10 volume of 3 M sodium acetate, 2 volumes of cold 95 % ethanol and incubating 20 minutes at – 20°C. DNA was spun down 15 minutes at 4°C, the pellet was dried and resuspended in 30 µl of the injection buffer (500 µl 10 mM KCl, 100 µl 10 mM NaH_2PO_4, 50 µl sterile green food colour, 350 µl distilled water).

2.3.2. Preparation of Microinjection Needles

The needles were prepared on horizontal micropipette puller (Sutter Instrument Company) using Capillary Glass Standard Wall Borosilicate Tubing With Filament (Sutter Instrument Company).

2.3.3. Preparation of Egg-Laying Plates and Agar-Coated Slides

4% bacto-agar in 200 mL of orange juice was boiled and poured into small petri dishes. Glass slides were dipped in the same mixture repeatedly until the thickness of the agar coat was at least 1 mm.

2.3.4. The Process of Injection and the Following Cross

Immediately after 30-minute egg collection, *yw* strain embryos were washed with 96% ethanol, aligned on microscope slide covered by 4% agar-orange juice media and the construct together with the helper plasmid was injected into the posterior pole of the embryo, where the primordial germ cells form. Injection was done through the chorion using a standard micromanipulator and borosilicate needles.

The injection had to be done within 60 minutes after the beggining of the embryo collection to be sure that the pole cells were not formed before injecton.

The embryos were raised at 25°C on the slides where they were injected, sealed in ampicillin medium plates (1% trypton, 1% NaCl, 0,5% yeast extract, 2% bacto-agar, 100 μg/mL ampicillin).

18-20 hours after injection, larvae started to hatch and they were transfered into vials containing regular food at a maximum density of 30 individuals per vial.

8.5 to 9 days after larvae collection, males and virgin females were individually crossed with *yw* flies. Their progeny with coloured (orange/red) eyes were mated with *yw*; *xa/CyO, MKRS* flies to map the new insertion to chromosome and to establish the transgenic stock (Fig. 2.2 and 2.3).

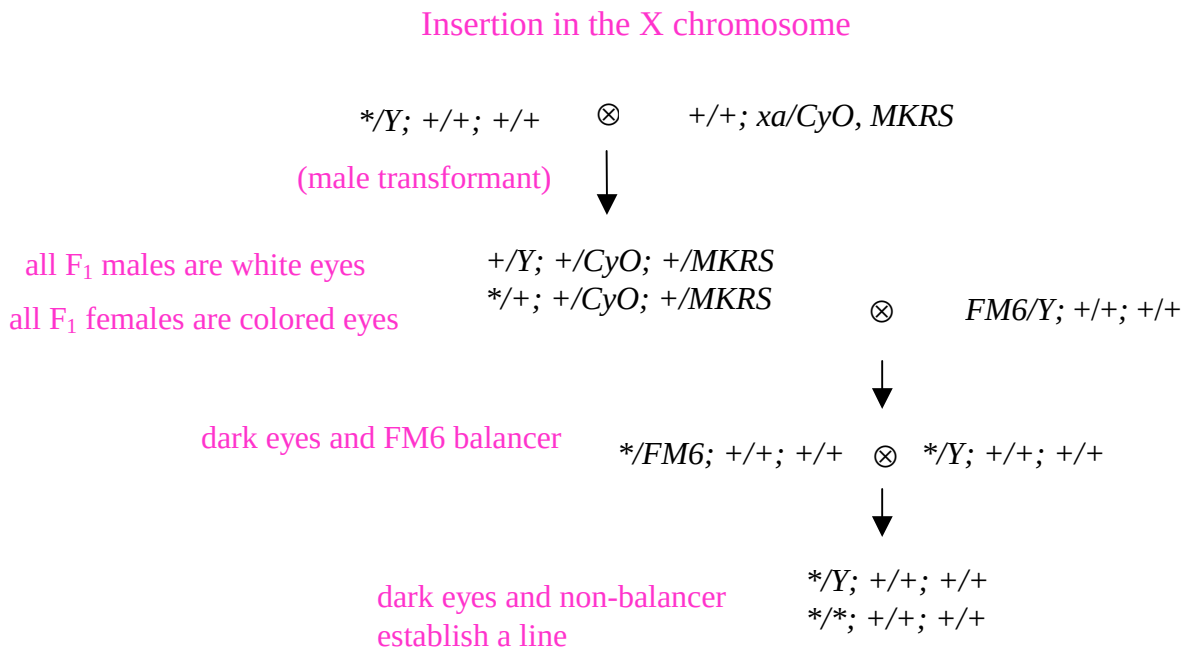

Fig. 2.2: Cross scheme in case of insertion in the X chromosome.

* stands for the *dco*-CTAP mutants. Since the pUAST-CTAP vector includes the mw^{+} marker, these mutant flies are distinguishable according to their red-colour eye. + represents the wild type chromosome.

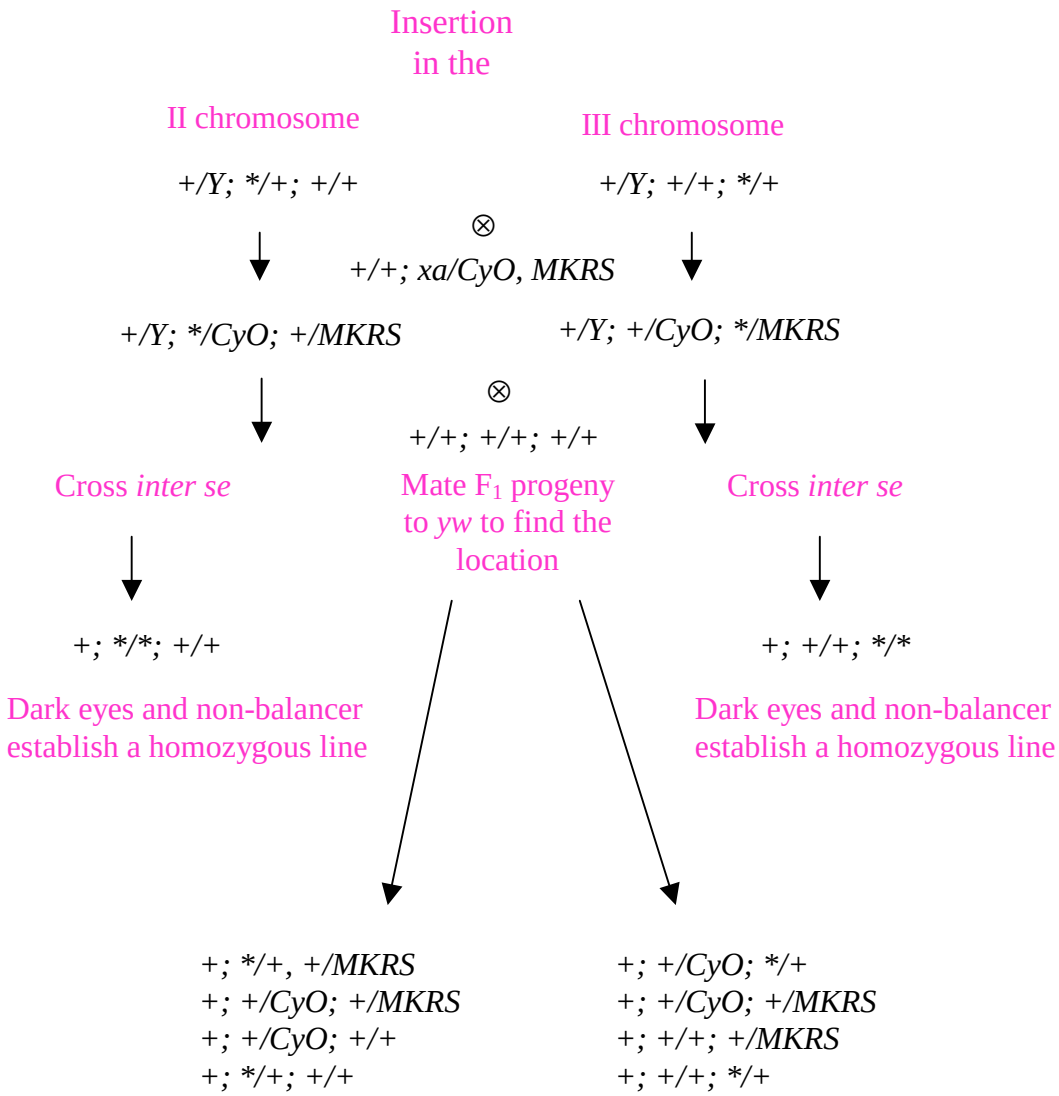

Fig. 2.3: Cross scheme in case of insertion in the II or III chromosome.
* stands for the *dco*-CTAP mutants. + represents the wild type chromosome.

2.3.5. Validation of Construct Incorporation into the Genome of Fruitfly

One fly was taken and squeezed in 50 µl of squishing buffer (10 mM Tris-HCl, pH 8.2; 1mM EDTA; 25mM NaCl; 200 µg/mL proteinase K (NEW ENGLAND BioLabs), freshly added). The reaction was incubated 30 minutes at 50°C and inactivated 2 minutes at 95°C. 1 µl was taken to the PCR reaction. For amplification, *Taq* DNA polymerase (TaKaRa) was used according to manufacturer´s instructions, except of the annealing temperature that was 68°C. Forward primer was complementary to the *dco* gene (Tab. 2.1); reverse to the CTAP region (SQ5; Tab. 2.2).

2.4. Multiple Insertion Test

During genome incorporation of the construct, multiple insertions in the scope of one chromosome could occur. According to the scheme below (Fig. 2.4), the simpliest screening is the control of the eye-colour type after two crosses to *yw*. The number of the eye colour nuances of F_2 generation implies the number of the chromosome insertions. If the males/females of the same age from F_2 generation share the same dark-eye-colour type, we can consider that only a single insertion has occurred. This information is useful for establishing of stable lines or for recombination events.

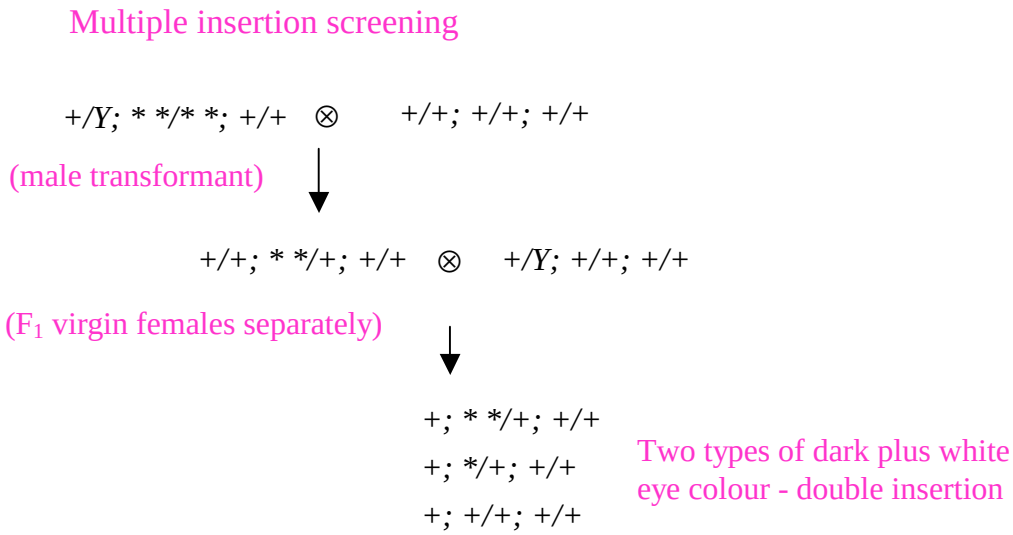

Fig. 2.4: Scheme of multiple insertion screening.

* stands for the *dco*-CTAP mutants, its number corresponds to the *dco*-CTAP insertion number. + represents the wild type chromosome.

2.5. The Genetic Rescue of Null *dco* Mutants

In order to determine, if the TAP-tagged *dco* gene insertion had been able to substitute the wild type *dco* alleles, the rescue experiment of null *dco* mutants was done according to the scheme in Fig. 2.5. The line carrying balanced *dco* lethal allele *dco[le88]* was crossed to the line carrying balanced chromosome deficiency *Df(3R)A177der22*, which includes the *dco* gene region. Both of the lines are not viable when homozygous. The desirable genotype (shown in the black box, Fig. 2.5) should therefore carry the disfunctional wild type *dco* gene in the III chromosome and the II chromosome could be used for pairing the TAP-tagged *dco* gene with appropriate Gal4 driver (in this case *arm* in the II chromosome). In such a scenario, Dco-CTAP protein would be expressed under *arm*-Gal4 driver in the absence of both wild type *dco* alleles.

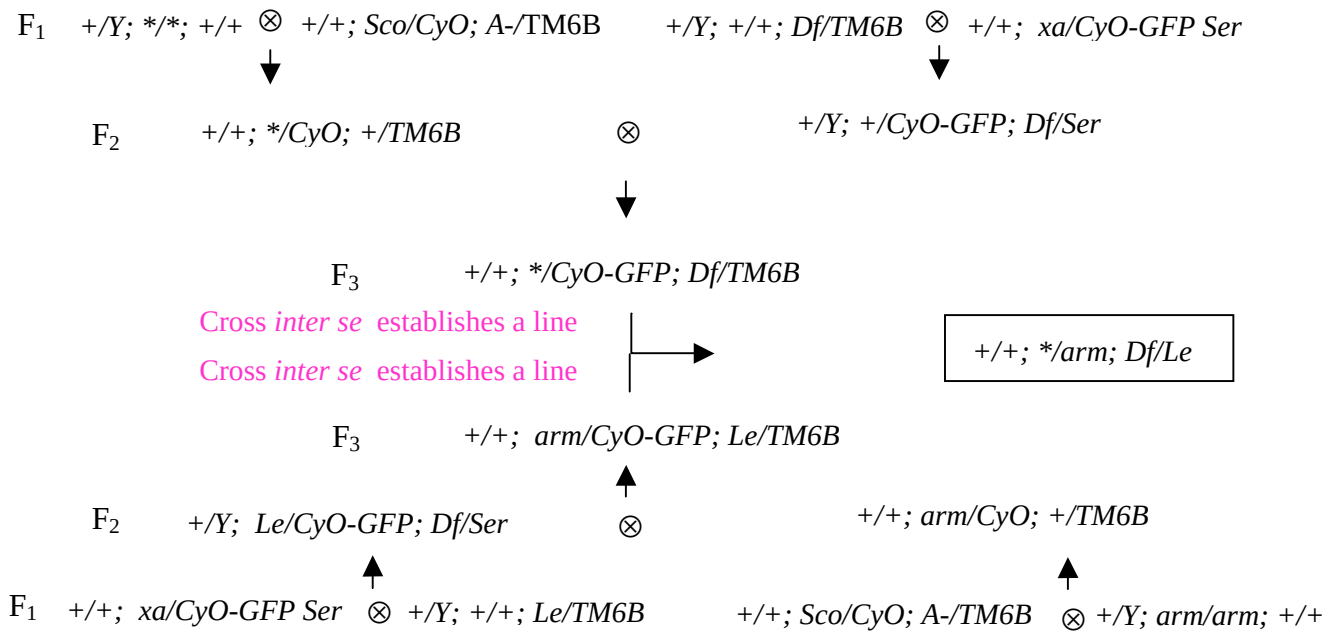

Fig. 2.5: Scheme of the genetic rescue of null *dco* mutants.
Le/TM6B is an abberation of the *FRT82 dco[le88]/TM6B Tb; Df/TM6B* of *Df(3R)A177der22 ry[+]/TM6B Tb*. * stands for the *dco*-CTAP mutants, + represents the wild type chromosome. The progeny of F_3 generation serve for the cross resulting in creation of the null *dco* mutant expressing the Dco-CTAP protein under the *arm*-Gal4 (shown schematically in the black box).

2.6. Defining of Targeted Expression of the Responder Gene

The initial characterization of five different Gal4s (Tab. 2.3) was done by crossing to a line containing a reporter gene UAS-Green Fluorescent Protein (GFP). Wandering third-instar larvae were collected and the green fluorescence was observed.

UAS-*dco*-CTAP lines were crossed to these Gal4s. Wandering third-instar larvae were collected and the expression of the tagged protein was checked on Western blotts using antibodies against the parts of the CTAP.

2.7. Preparation of Cell Lysates and Western Blotting

Wandering larvae were homogenized in 50 µl of 1x Sample Buffer (50 mM Tris-HCl, pH 6.8; 2% sodium dodecyl sulfate (SDS); 100 mM dithiothreitol (DTT); 10% glycerol). The lysate was boiled at 95°C for 5 minutes and spun down at 4°C for 10 minutes. 10 µl of these lysates were resolved on 12% or 15 % SDS-PAGE gel. The prestained Precision Plus Protein Standard (Bio-Rad) was run simultaneously.

Proteins were transferred to a nitrocellulose membrane (BioTrace^{TM} NT, PALL Life Science) by electroblotting using the Extra Thick Blot Paper (BioRad), Transfer Buffer (10 mM $NaCHO_3$, 3 mM Na_2CO_3 in 20% metanol, pH 9.9) and Trans_Blot SD Semi-Dry Transfer Cell (Bio-Rad).

The membrane was stained with 1x Ponceau reagent to confirm transfer. The stain was washed off with 1x PBST (138 mM NaCl, 1.5 mM KH_2PO_4, 8 mM Na_2HPO_4, 3 mM KCl, 0.05% Tween-20). The membrane was blocked overnight with 5% milk in 1x PBST at 4°C. Next day, it was incubated by shaking for 2 hours at room temperature with a primary antibody diluted in 5% milk in 1x PBST (Tab. 2.4).

Tab. 2.4: List of used primary antibodies.

Primary antibody	Developed in	Dilution
Anti-Protein A (Sigma)	rabbit	1:2000
Anti-Calmodulin Binding Peptide (Immunology Consultants Laboratory)	rabbit	1:2000

The membrane was washed with 1xPBST 3 times by shaking for 10 minutes and incubated for 2 or 4 hours in 5% milk in 1x PBST with 1:2000 secondary anti-rabbit antibody conjugated to horseradish peroxidase (Jackson ImmunoResearch Laboratories). The membrane was washed again 3 times by shaking with 1xPBST for 10 minutes. The signal was

visualized using the ECL Kit (Pierce) according to the supplied protocol. Blots were exposed in MF-ChemiBIS (DNR Bio-Imaging Systems Ltd.).

2.8. Tandem Affinity Purification

Tandem affinity purification (TAP) is a procedure for purification of proteins expressed under native conditions. Introduction of two different affinity purification steps greatly enhances the specificity of the purification procedure.

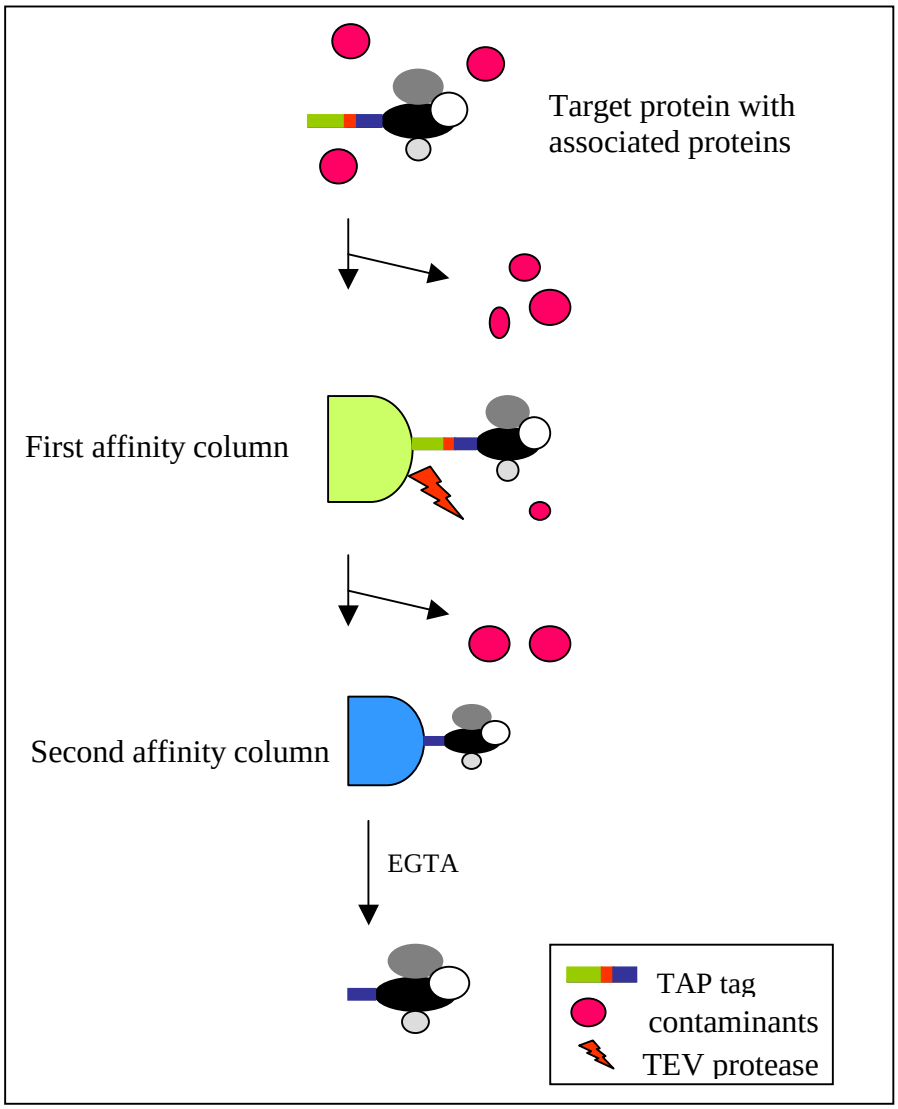

Fig. 2.6: Scheme of the tandem affinity purification.

This method is based on two subsequent affinity chromatography steps. The TAP tag, fused to a carboxy- or amino-terminus of the target protein, is composed of protein A having very high affinity for Immunoglobulin G (IgG), a TEV protease cleavage site and calmodulin binding peptide (CBP) having high affinity for calmodulin. An extract containing the

TAP-tagged target protein is mixed with IgG affinity resin before being incubated with TEV protease that releases the target protein by cleavage. This eluate is used for a second affinity step. The target protein is bound to calmodulin in the presence of calcium before release of the purified complex by ethylene glycol tetraacetic acid (EGTA) chelating calcium ions essential for calmodulin binding (Fig. 2.6).

2.8.1. TAP Procedure

For protein extraction, a detergent-based lysis buffer was used (50 mM Tris, pH 7.5; 125 mM NaCl; 5% glycerol; 0.2–0.4% NP-40; 1.5 mM $MgCl_2$; 1 mM DTT; 25 mM NaF; 1 mM Na_3VO_4; 1 mM EDTA; Complete protease inhibitor from Roche), (Veraksa at al., 2005). Approximately 3 000 wandering larvae were collected and homogenized in this lysis buffer at 4°C. After a 20-minute incubation on ice, larvae extracts were cleared by centrifugation at 20 000 x g for 15 min. Supernatants were frozen in liquid nitrogen and stored at -80°C.

The following steps were executed according to Puig et al., 2001 with slight modifications. Binding and elution steps were done in 0.8 x 4 cm Poly-Prep columns (Bio-Rad). Two hundred microliters of IgG Sepharose 6 Fast Flow beads (GE Healthcare Life Science), corresponding to 400 µl of bead suspension, were transferred into the column. The beads were washed twice with 10 ml IPP150 (10 mM Tris–Cl, pH 8.0; 150 mM NaCl; 0.1% NP-40). pH on the column was checked using a lacmus paper. Then the extract was transferred into the column containing the washed beads and rotated for 4 h at 4°C.

Elution was done by gravity flow and the beads were washed three times with 10 ml of IPP150 and once with 10 ml of TEV cleavage buffer (IPP150 adjusted to 0.5 mM EDTA and 1 mM DTT). Cleavage was done in the same column by adding 2 ml of TEV cleavage buffer and 200 units of AcTEV protease (Invitrogen). The beads were rotated overnight at 4°C and the eluate was recovered by gravity flow.

One hundred microliters of Calmodulin Affinity Resin (Stratagene), corresponding to 200 µl of bead suspension, was transferred into a column and washed twice with 10 ml of IPP150 calmodulin binding buffer (10 mM Tris–Cl, pH 8.0; 10 mM 2-mercaptoethanol; 150 mM NaCl; 1 mM magnesium acetate; 1 mM imidazole; 2 mM $CaCl_2$; 0.1 % NP-40).

6 ml of IPP150 calmodulin binding buffer and 6 µl of 1 M $CaCl_2$ were added to the 2 ml of eluate recovered after TEV cleavage. This solution was transferred to the column containing washed calmodulin beads and rotated for 3.5 h at 4°C. After the beads were washed with 30 ml of IPP150 calmodulin binding buffer, the bound proteins were

eluted with 1 ml of IPP150 calmodulin elution buffer (10 mM Tris–Cl, pH 8.0; 10 mM 2-mercaptoethanol; 150 mM NaCl; 1 mM magnesium acetate; 1 mM imidazole; 0.1% NP-40; 2 mM EGTA).

2.8.2. Analysis of the Recovered TAP Eluate

Recoved material was separeted into halves and precipitated overnight at -20°C using 4V of cold acetone. One part was resuspended in 100 mM ammonium bicarbonate, pH 8.5. 2 µl of trypsin (Sigma) solution (1mg/mL trypsin in 1 mM HCl) were added and the digestion was done over night at 37°C.

Another part was resuspended in 25 µl 1x Sample Buffer and 12.5 µl was loaded on 12 or 15% SDS-PAGE. Staining was done using SYPRO Ruby Protein Gel Stain (Invitrogen).

Bands of interest were cut out from the gel. Gel pieces were twice covered with 200 µl of ammonium bicarbonate with 40% acetonitrile and incubated at 37°C for 30 minutes. The solution was discarded and the samples were dried in a SpeedVac for approximately 15 minutes. 0.4 µg of trypsin in 1 mM HCl and 68 µl of 40 mM ammonium bicarbonate in 9% acetonitrile was added to the gel piece and incubated overnight at 37°C.

2.9. Mass Spectrometry (MS) Analysis

Prior to mass spectrometry analysis, the samples were purified either by filtration on Microcon Ultracel YM-10 centrifugal filter devices with a molecular weight cut-off of 10 000 (Millipore), or using the Zip Tip C18 pipette tips (Millipore).

Mass spectra were obtained on a LC-MS/MS system based on ultra performance liquid chromatography (UPLC) operating in nano-flow regime (nano Acquity, Waters) coupled to a qTOF Premier mass spectrometer (Waters). A linear gradient of water/acetonitril was used for the peptide separation on the reverse phase nanoACQUITY UPLC BEH300 C18 Column, 1.7 µm bead diameter, 75 µm x 150 mm, 10K psi (Waters).

The UPLC gradient started at 3% ACN, linearly increased to 60% during 35 minutes, then increased to 85% for the next 5 minutes. After the washing step the concentration of ACN returned to the initial 3% for the rest of the 60 minute run.

Two different methods were used to obtain raw mass spectra, MS Survey and MS^E Identity (Waters).

MS Survey is also known as Data Dependent Analysis (DDA). MS spectrum is obtained during the whole 60 minute LC run in low collision energy (5V) mode. When a precursor (a peptide) is detected, the system switches to MS/MS, increases the collision

energy (20 - 40V) and fragment spectrum is measured for the selected precursor. The peptide is detected as an increase in the total ion count. After the ion count decreases under 10 counts per second, the system switches back to MS survey. The system is set to measure 3 different fragment spectra simultaneously, if necessary.

Running the MS^E Identity (Waters) method, the system does not switch between low-energy MS spectrum measurement and high-energy fragment MS/MS spectrum measurement. The low-energy data (5V) and elevated energy (20 - 40V) data are collected simultaneously; precursor ions and their fragments are matched based on their LC retention time by the Apex3D (Waters) algorithm during raw data processing.

The resulting raw data were processed using the ProteinLynx 2.3 Browser (PLGS 2.3) software (Waters). Database searches were performed using the same software. Protein databases were downloaded from the NCBI site (http://www.ncbi.nlm.nih.gov). The spectra were compared to a general database and to a specific *D. melanogaster* database.

2.10. Prediction of CKI Phosphorylation Sites

Prediction of post-translational phosphorylation of CKI from the amino acid sequence was done using NetPhospK 1.0 Server (Blom et al., 2004).

3. Results

3.1 Generation of *dco*-CTAP pUAST Vector

The PCR product of expected size (*dco* coding sequence, 1322 bp) was subcloned into the pGEM T-easy vector. The insert was cut out by *Xho I* and *Kpn I* restriction enzymes and cloned into the pUAST-CTAP vector. The coding region of the *dco* gene without the stop codon was introduced in-frame with the C-terminal TAP tag.

Control of the correct insert incorporation was done by restriction reaction of *dco*-CTAP pUAST vector, using *Xho I* and *Kpn I* enzymes (Fig. 3.1), and by sequencing of the *dco*-CTAP region (see Material and Methods, Chapter 2.1).

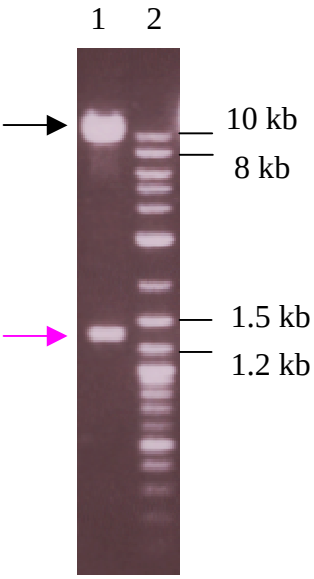

Fig. 3.1: Product of the restriction reaction (*Xho I/ Kpn I*) of *dco*-CTAP pUAST.
1- The upper band, marked with black arrow, corresponds to the size of CTAP pUAST vector sequence of 9627 bp, and the lower band, marked with pink arrow, corresponds to the size of the *dco* coding sequence of 1322 bp; 2 – ladder.

3.2. Generation of Transgenic Flies

Approximately 1050 *yw* embryos were injected with the *dco*-CTAP pUAST construct together with the helper P-element plasmid pπ25.7wc (Fig. 3.2).

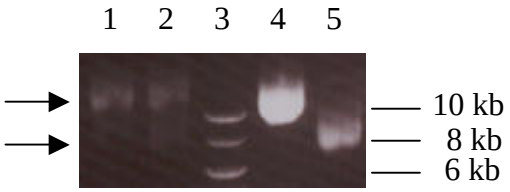

Fig. 3.2: The mix of plasmids used for the injection of *Drosophila* embyos.
1 - 2 The mix of the *dco*-CTAP pUAST and pπ25.7wc vector, each of them marked with black arrow; 3 - ladder; 4 - *dco*-CTAP pUAST vector; 5 - pπ25.7wc vector.

Bacause of the relatively small size of the construct (~11 kb), incorporation into the genome was highly effective. Thus after individual male and virgin female cross to *yw* flies, only some progeny with coloured (orange/red) eyes was kept.

24 coloured flies were mated with *yw*; *xa/CyO, MKRS* flies to map the new insertion to chromosome and to establish the transgenic stock (see Material and Methods, Fig. 2.2 and 2.3). 2 lines with insertion in the X chromosome, 13 in the II and 9 in the III were obtained (Tab. 3.1).

Tab 3.1: The list of stable lines kept for futher experiments.

Characterization	Stock code	Balancer
Insertion in the X chromosome	OL-4, D5	*TM6*
Insertion in the II chromosome	II5, CH9, 42/1, CH13, 4X, N, N10, 40, CH1	*CyO*
Insertion in the III chromosome	N9, H5, 20A, CH7, 20, H8, 62	*MKRS*

3.3. Lines Characterization

Three different lines with the insertion in the II and three in the III chromosome were tested for the number of insertions in one chromosome according to the Material and Methods, Chapter 2.4. Two lines (II chromosome insertion) exhibited the same dark-eye-colour type of

males/females of the same age in F_2 generation indicating single insertion. The other exhibited two types of dark eye colour indicating double insertion.

3.4 The Construct Was Incorporated into the Genome of Fruitfly

Genome incorporation of the construct was validated by the PCR reaction done on fly homogenate (Matrial and Methods, Subchapter 2.3.5). We could take the advantege of the tag fused to the *dco* gene in order to differentiate the original *dco* sequence present in fly genome from the sequence randomly incorporated during embryo injection. Forward primer was complementary to the *dco* gene and reverse to the CTAP region. The expected size of the amplified product was 1379 bp.

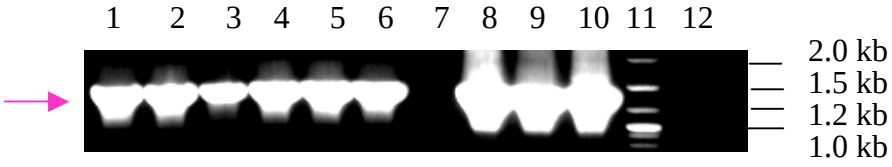

Fig. 3.3: Validation of construct incorporation into the fruitfly genome.
1, 2 - lines with ´X inserton´; 3, 4 - lines with ´II inserton´; 5, 6 - lines with ´III inserton´;
7 - *yw*, negative control; 8 – 10 different *dco*-CTAP pUAST plasmids, positive control; 11-ladder; 12 - PCR done with H_2O instead of DNA, negative control. Pink arrow marks amplified product of 1379 bp.

3.5. Tagged Dco Protein is Expressed under Different Gal4

To verify the expression of tagged Dco protein in wandering third-instar larvae, Western blot analysis using Anti-Protein A primary antibody was performed. Two different lines (OL-4 and 40 - Tab. 3.1) were crossed to five Gal4 to compare the level of Dco expression. *arm*, 339, 340, 560 and 1018 are the stock codes of used Gal4s (Tab. 2.3) corresponding to the abbreviation *arm*-Gal4, 339-Gal4, 340-Gal4, *act*-Gal4 used in following text.

Line OL-4 exhibited higher expression level than line 40 under all 5 drivers (data not shown) and at both cases the highest expression level was observed under *act*–Gal4 and 560-Gal4 (Fig. 3.4). Without any Gal4, a slight background expression was seen.

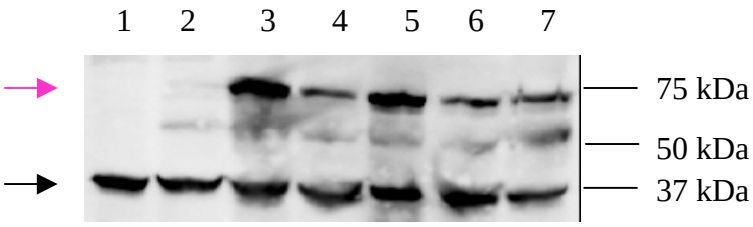

Fig. 3.4: Level of expression of Dco-CTAP protein under different Gal4s.
1 - *yw*, negative control; 2 – transgenic line *dco*-CTAP (OL-4); 3 - OL-4 under 560-Gal4; 4 - OL-4 under 340-Gal4; 5 - OL-4 under *act*-Gal4; 6 - OL-4 under *arm*-Gal4; 7 - OL-4 under 339-Gal4. The upper bands marked with pink arrow, correspond to the fusion Dco-CTAP protein of 68,9 kDa. The lower band marked with black arrow, which is seen also in the negative control, is a nonspecific protein of 37 kDa. The band between, which is not seen in the negative control, may be a degradation product of the Dco-CTAP protein.

Three different Gal4 (*act*, *arm* and 560) were used for the cross with OL-4 and 40 line and futher larval collection. When a homozygote mutant virgine female was crossed to a heterozygous *act-Gal4/TM6B Hu Tb* male, less than one half of the wandering third-instar larvae segregated with *act*-Gal4. The strong *act*-Gal4 Dco over-expression affects the development of the fly, and although larvae under *act*-Gal4 exhibited the strongest expression, the final larval-mass volume was not sufficient enough. Both of the *arm*-Gal4 (lower expression) and 560-Gal4 (stronger expression) were tested in order to compare results of the tandem affinity purification from two lines with a different over-expression level of Dco.

3.6. The Dco-CTAP Rescues 86.7 % of the Null *dco* Mutants

Dco-CTAP protein was expressed under *arm*-Gal4 driver in the absence of both wild type *dco* alleles according to the Material and Methods, Chapter 2.5. For the rescue experiment, homozygous mutant flies of *dco*-CTAP and *arm*-Gal4 were crossed in order to obtain the progeny, where *dco*-CTAP is guided by *arm*-Gal4 in every larvae. The heteroallelic combinations of *[le88]* and of *dco* deficiencies result in the death during the larval stages (Zilian et al., 1999). The heterozygous mutants of *dco*-lethal *[le88]* balanced with *TM6B* and of *dco*-deficiency *Df(3R)A177der22* balanced with *TM6B* were crossed.

Since the *TM6B/TM6B* combination was not viable, the expected ratio between the null *dco* mutants and the *dco[le88]/TM6B* plus *Df(3R)A177der22/TM6B* larvae is 1:2. We

obtained the 86,7% of *dco*-CTAP/*arm*-Gal4, *dco[le88]/Df(3R)A177der22* pupae (scoring 400 pupae), indicating that the tagged Dco is able to rescue the *dco* null mutant.

3.7. Tandem Affinity Purification

3.7.1. The Efficiency of the First Purification Step is Low

To test efficiency of the first affinity purification step, a lysate of approximately 600 wandering larvae (OL-4 insertion under *arm*-Gal4) was loaded on IgG column. After several washing cycles, the Dco-CTAP fussion protein was released from the column via treatment with solution of low pH (0.5 M HAc, pH 3.4). Large amount of the fussion protein in the flow-through fraction indicates low binding affinity of the protein to the IgG matrix (lane 2, Fig. 3.5). Althogh, loss of the fusion protein during flow-though stage was considerable, the amount of the Dco-CTAP protein trapped on the IgG matrix (lane 5, Fig. 3.5) was sufficient allowing the second affinity purification step.

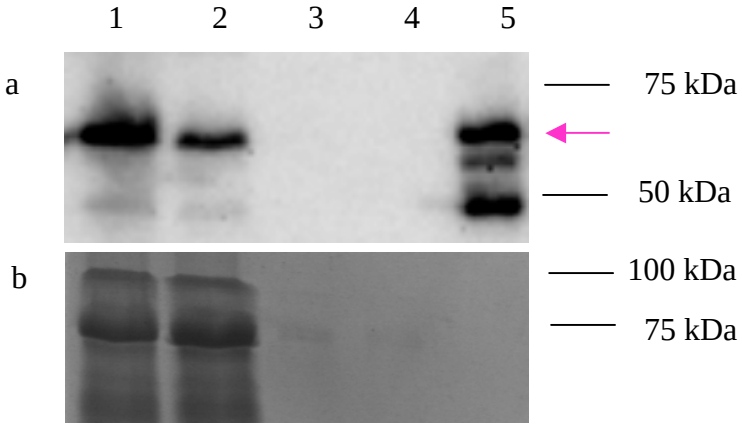

Fig. 3.5: Test of the first binding step (IgG matrix).
a – Western blot using Anti-Protein A antibody, b – Coomasie stained 12% SDS-PAGE shown as a loading control. 1 - load on column; 2 – flow through; 3, 4 – wash steps; 5 – elution. The upper bands marked with pink arrow, correspond to the fusion Dco-CTAP protein of 68,9 kDa.

3.7.2. The Efficiency of the Second Purification Step is Insufficient

To test the binding efficiency of the second affinity column, a lysate from approximately 3 000 wandering larvae (OL-4 insertion under 560-Gal4) was collected and loaded on the IgG matrix. The fussion Dco protein was released from IgG matrix by AcTEV protease cleavage.

The eluate was used in the second affinity purification step comprising of the calmodulin matrix. Comparison of the amount of tagged Dco detected among load control, flow-though, wash and elution fractions indicated very low efficiency of the fusion protein binding to the calmodulin matrix (Fig. 3.6).

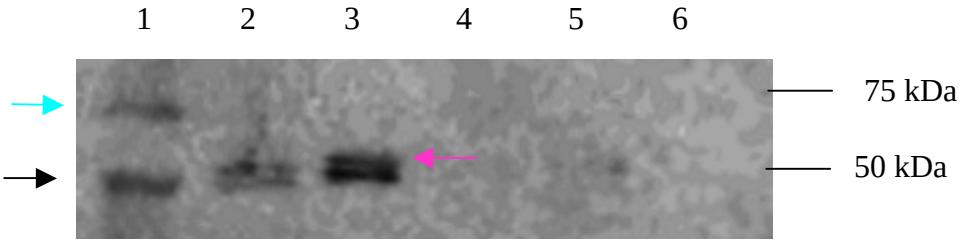

Fig. 3.6: Test of the second binding step (calmodulin matrix).
Western blot using Anti-CBP antibody. 1 – IgG matrix after cleavage; 2 – eluate of the first column using AcTEV protease; 3 – flow through of the second column, 4 – first wash steps; 5 – calmodulin beads, 6 – second wash step. Band marked with light blue arrow, corresponds to the fusion Dco-CTAP protein of 68,9 kDa. Bands, marked with pink arrow correspond to the fusion CBP-Dco protein of 52 kDa, bands marked with black arrow correspond to IgG heavy chain of 50 kDa.

One half of each sample of the recovered and acetone-precipitated TAP eluate was resuspended in 25 µl 1x Sample Buffer and 12,5 µl was resolved on 12% SDS-PAGE (Fig. 3.7). These final eluates were extremely low-concentrated. To compare, see the abundance of signal resulting from the 125 ng of enolase (lane 5). Approximately 3 000 wandering larvae of OL-4 and 40 line under 560-Gal4 were culled and homogenized. Lysates of the same initial protein concentration were used for TAP. As a negative control, the whole procedure using the lysate of the approximately 3 000 wandering 560-Gal4 larvae of the same initial protein concentration was run simultaneously.

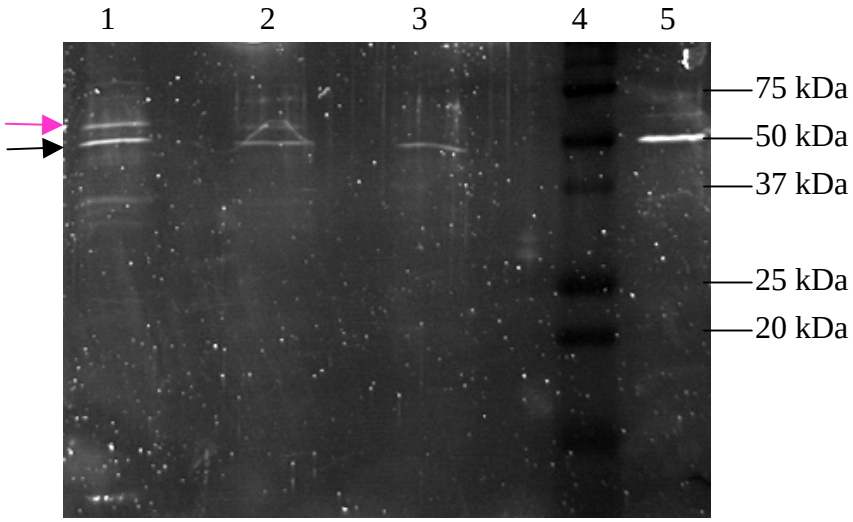

Fig. 3.7: Elution of the calmodulin column.

SYPRO Ruby stained 12% SDS-PAGE. 1 - positive sample (OL-4 x 560 cross); 2 - positive sample (40 x 560 cross); 3 - negative sample (560, control); 4 - marker; 5 – Yeast enolase (Sigma) of known concentration (125 ng) as a stain intensity control. Bands, marked with pink arrow correspond to 52 kDa of the Dco protein fused with the remaining calmodulin binding peptide (CBP) sequence, bands marked with black arrow correspond to the contaminant (Fat body protein 1).

3.8. Identification of the Purified Proteins

The second part of the final TAP-eluate was trypsin digested and MS spectra of each sample were aquired at least three times (Material and Methods, Chapter 2.9) using both MS^E and Survey scan technigues. Totally, four proteins were identified; Dco, Heat shock protein cognate 4, β-spectrin, Fat body protein 1 (Fbp 1). Dco, Heat shock protein cognate 4 and β-spectrin are considered as a positive hits (Tab. 3.2, corresponding to the first and the second lane of Fig. 3.7). Fbp 1 (CG17285) is considered as a contaminant as it was present also in TAP-eluate of the sample of 560-Gal4 larvae lysate. Peptides of trypsin were found as well. If the protein sample is low- concentrated, trypsin starts to digest itself and MS analysis identifies also resulting peptides.

Tab. 3.2: Tandem affinity purified proteins of *D. melanogaster* and characterized with at least three different peptides by MS analysis.

Description – name (symbol) and comment according to the Flybase.org
Discs overgrown protein kinase, CG2048; + one peptide sequence of CBP part of the TAP tag
Heat shock protein cognate 4 (Hsc70-4) CG4264 Its molecular function is described as: ATPase activity; unfolded protein binding; chaperone binding; ATP binding. It is involved in the biological processes: embryonic development via the syncytial blastoderm; axon guidance; axonal fasciculation; nervous system development; neurotransmitter secretion; vesicle-mediated transport; protein folding; RNA interference.
β-spectrin, CG5870 Its molecular function is described as: cytoskeletal protein binding; actin binding; actin filament binding; calmodulin binding; microtubule binding; phosphatidylinositol-4,5-bisphosphate binding; structural constituent of cytoskeleton. It is involved in the biological processes described with 11 unique terms, many of which group under: synaptic transmission; anatomical structure development; regulation of cellular component organization and biogenesis; cell-cell signaling; cell projection organization and biogenesis; organelle organization and biogenesis; cell motion; neuron differentiation; cell morphogenesis; neurotransmitter transport; fusome organization and biogenesis; regulation of developmental process; plasma membrane organization; biogenesis.

Because of the high loss during the second purification step, the MS analysis was also performed on the samples recovered after the AcTEV protease cleavage. Since a high number of contaminants was detected, the evaluation of the results from MS analysis was performed via comparison of two datasets (positive and negative). Proteins present in both datasets were subtracted. The list of Dco-CTAP copurified proteins resulting from three different purification procedures served as a positive dataset. The list of proteins interacting nonspecifically (using 560-Ga4 larval lysate) with the IgG matrix resulting from three different purification procedures served as a negative dataset.

The resulting list of proteins identified together with the Discs overgrown protein kinase (CG2048) is shown in Tab. 3.3. The confidence values of the MS analysis of proteins listed in Tab. 3.2 and Tab. 3.3 are listed in Appendix (Tab. A1-A3).

Tab. 3.3: Dco-copurified proteins of *D. melanogaster* using the IgG matrix and characterized with at least three different peptides by MS analysis.

Description - name (symbol) and comment according to the Flybase.org
Heat shock protein cognate 4 (Hsc70-4) CG4264 Described in Tab. 3.2.
CG34356 Its molecular function is described as: protein kinase activity; ATP binding; DNA binding. It is involved in the biological processes: DNA methylation; protein amino acid phosphorylation.
The gene lethal (1) G0156, CG12233 PA Its molecular function is described as isocitrate dehydrogenase (NAD+) activity. It is involved in the biological process of tricarboxylic acid cycle.
Mushroom body defect protein (Mud) CG12047 Its molecular function is described as: steroid hormone receptor activity; superoxide dismutase activity; transcription factor activity; metal ion binding. It is involved in the biological processes: spindle assembly involved in female meiosis II; mushroom body development; superoxide metabolic process; regulation of transcription.
Fak-like tyrosine kinase (PR2) CG3969 PB Its molecular function is described as: protein tyrosine kinase activity; non-membrane spanning protein tyrosine kinase activity; ATP binding; serine-type peptidase activity; calcium ion binding. It is involved in the biological processes: protein amino acid phosphorylation; autophagic cell death; salivary gland cell autophagic cell death; proteolysis.
CG4290 PA Its molecular function is described as: protein serine/threonine kinase activity; ATP binding. It is involved in the biological process of protein amino acid phosphorylation.
Hook protein (Hk) CG10653 Its molecular function is described as microtubule binding. It is involved in the biological processes: determination of adult life span; endocytosis; cytoskeleton-dependent intracellular transport; endosome transport; R7 cell development; phagocytosis, engulfment; microtubule cytoskeleton organization and biogenesis.
Shibire (Shi) CG18102 Its molecular function is described as: actin binding; microtubule binding; microtubule motor activity; GTPase activity; GTP binding. It is involved in the biological processes described with 28 unique terms, many of which group under: transport; reproductive process in a multicellular organism; anatomical structure development; mating; learning and/or memory; endocytosis; organelle organization and biogenesis; regulation of biological process; system process; open tracheal system development; cell motion; synaptic vesicle endocytosis.

Tab. 3.3: Continued.

Description - name (symbol) and comment according to the Flybase.org
Probable phenoloxidase subunit, CG8193 Its molecular function is described as: monophenol monooxygenase activity; oxygen transporter activity. It is involved in the biological processes: defense response; metabolic process; transport.
Dynein heavy chain 64C, CG7507 PB Its molecular function is described as: ATPase activity; microtubule motor activity; motor activity; ATP binding; cysteine-type endopeptidase activity. It is involved in the biological processes described with 31 unique terms, many of which group under: organelle organization and biogenesis; cell cycle; anatomical structure development; cell cycle process; transport; cellular localization; RNA localization; fusome organization and biogenesis; microtubule-based movement; macromolecule localization.
Dynein heavy chain at 62B (Dhc62B) CG15804 PB Its molecular function is described as: motor activity; ATPase activity; ATP binding; microtubule motor activity. It is involved in the biological process of microtubule-based movement.
CG14438 PA Its molecular function is described as zinc ion binding. The biological processes in which it is involved are not known.
CG5794 PB Its molecular function is described as ubiquitin thiolesterase activity. It is involved in the biological process of ubiquitin-dependent protein catabolic process.
CG14967 PA Its molecular function is unknown. The biological processes in which it is involved are not known.
Nahoda protein, CG12781 PA Its molecular function is described as dopamine beta-monooxygenase activity. It is involved in the biological process of histidine catabolic process.
Topoisomerase 3α, CG10123 Its molecular function is described as: DNA topoisomerase type I activity; DNA topoisomerase activity; zinc ion binding. It is involved in the biological processes: DNA topological change; DNA unwinding during replication.
CG14438 PB Its molecular function is described as zinc ion binding. The biological processes in which it is involved are not known
v(2)k05816, CG3524 PA Its molecular function is described by 3-oxoacyl-[acyl-carrier-protein] synthase activity; [acyl-carrier-protein] S-acetyltransferase activity; [acyl-carrier-protein] S-malonyltransferase activity; hydrolase activity, acting on ester bonds; acyl carrier activity; zinc ion binding; oxidoreductase activity; cofactor binding. It is involved in the biological processes: oxidation reduction; biosynthetic process.

Tab. 3.3: Continued.

Description - name (symbol) and comment according to the Flybase.org
CG1024 Its molecular function is described as zinc ion binding. The biological processes in which it is involved are not known.
Rugose (rg) CG6775 Also known as A kinase anchor protein 550 (AKAP 550). Its molecular function is described as protein kinase A binding. It is involved in the biological processes: protein localization; compound eye cone cell differentiation.
GTPase activating protein (CdGAPr) CG10538 Its molecular function is described as GTPase activator activity. It is involved in the biological process of signal transduction.
Proteasome p44.5 subunit (Rpn6) CG10149 Its molecular function is described as endopeptidase activity. It is involved in the biological process of proteolysis.
CG6985 PA Its molecular function is unknown. The biological processes in which it is involved are not known.
Brakeless protein, CG5580 Also known as scribbler. Its molecular function is described as: transcription factor activity; zinc ion binding; phosphopantetheine binding. It is involved in the biological processes: axon target recognition; axon guidance; larval locomotory behavior; negative regulation of transcription from RNA polymerase II promoter; photoreceptor cell development; regulation of imaginal disc growth; imaginal disc-derived wing morphogenesis; negative regulation of specific transcription from RNA polymerase II promoter.
CG34417 PC Its molecular function is described as: structural constituent of cytoskeleton; actin binding. It is involved in the biological process of mesoderm development.
CG7156 PA Its molecular function is described as: protein kinase activity; ATP binding; protein binding; phosphoinositide binding. It is involved in the biological processes: cell communication; protein amino acid phosphorylation.
CG7943 Its molecular function is described as: transmembrane transporter activity. It is involved in the biological process of transport.
Crooked neck (crn) CG3193 PA Its molecular function is described as binding. It is involved in the biological processes: nuclear mRNA splicing, via spliceosome; Malpighian tubule morphogenesis; central nervous system development; neuroblast proliferation; peripheral nervous system development; regulation of alternative nuclear mRNA splicing, via spliceosome; neuron fate commitment.
CG13618 PA Its molecular function is unknown. The biological processes in which it is involved are not known.

Tab. 3.3: Continued.

Description - name (symbol) and comment according to the Flybase.org
CG1677 Its molecular function is described as: zinc ion binding; nucleic acid binding. The biological processes in which it is involved are not known.
Chromosome-associated protein (Cap) CG9802 PB Its molecular function is described as: ATP binding; protein binding; ATPase activity. It is involved in the biological processes: sister chromatid cohesion; chromosome organization; biogenesis.
CG17282 PA Its molecular function is described as binding. The biological processes in which it is involved are not known
CG4140 Its molecular function is unknown. The biological processes in which it is involved are not known.
Chitinase 3 (Cht3) CG18140 Its molecular function is described as: chitinase activity; cation binding; chitin binding. It is involved in the biological process of cuticle chitin catabolic process.

4. Discussion

The coding region of the *dco* gene was cloned into the pUAST-CTAP vector. Transgenic fly lines carrying *dco*-CTAP in the X, II and III chromosome were generated and characterized. The overexpression of tagged Dco protein was obtained under different Gal4 drivers. The strongest overexpression in the wandering larvae resulted from the use of *act*-Gal4. However, such high level of Dco expression negatively affected the larval development. Driver 560-Gal4 aiming an expression of the target protein to the imaginal discs exhibited sufficient level of Dco expression withough affecting the larvae.

Larvae expressing Dco-CTAP under *arm*-Gal4 driver in the background of larval lethal heteroallelic combinations of *dco* lethal allele *[le88]* and of *dco* deficiency *Df(3R)A177der22* were viable and were able to pupariate. Thus the tagged Dco protein was able to substitute its wild type form during larval development, which suggests that the tagged protein is (at least partially) functional.

The limiting step of the whole methodological strategy was the tandem affinity purification. The minimal amount required for MS analysis is approximately 75 ng. Eventhough the inputting larval lysate of each experiment had been increased up to 10 mL (corresponding to minimally 3000 homogenized larvae), the resulting Dco-CTAP protein concentration was extremely low reaching detection limit for MS analysis. Although modifications of the incubation time and amount of IgG beads had been tested, the protein A (protA) part of the TAP tag did not bind effectively to the IgG matrix. Low binding affinity was also observed in a case of the calmodulin binding peptide (CBP) and calmodulin beads. The low efficiency of the whole TAP procedure was also marked by low AcTEV protease cleavage efficiency which was low regardless the incubation time and different temperature settings. For further experiments, the use of another affinity system could be taken into consideration. In mammalian cells, the TAP method also suffers from a low overall yield. Bürckstümmer et al., 2006 compared the efficiency of other alternative dual-affinity tags optimalized for use in mammalian cells. For example, the tag based on protein G and streptavidine-binding peptide (GS-TAP) resulted in a tenfold increase in protein-compex yield and improved the specifity of the procedure as compared to protA and CBP-TAP.

The sequence of both TAP steps should remove the copurified artifacts. We observed only four proteins eluated out off the calmodulin column. Totally, four proteins were identified; Dco, Heat shock protein cognate 4, β-spectrin and Fat body protein 1. Dco, Heat

shock protein cognate 4 and β-spectrin could be considered as a positive hits. β-spectrin is known substrate of casein kinase (CKI). It has been demonstrated *in vivo* experiment by Boivin, 1988 that purified casein kinases are able to phosphorylate *in vitro* the β chain of purified spectrin with [γ-32P]ATP as a phosphoryl donor. β-spectrin phosphorylation by CKI has been shown to decrease membrane mechanical stability (Manno et al., 1995). Moreover the tandem affinity purification coupled to mass spectrometry applied to all ORFs of *Saccharomyces cerevisiae* revealed the interaction between the Dco ortholog Hrr25 and Hsc70-4 ortholog SSA1 (Gavin et al., 2006). These facts indicate that our two positive hits, Hsc70-4 and β-spectrin, can be considered as true Dco interactors.

The low affinity of both parts of the tag to its matrix (as mentioned above) might result from sterical hindrance of the tag. Certain portion of Dco-CTAP protein could have been hidden inside a multiprotein complex under native conditions. In such scenario, tag would not be able to bind efficiently to the affinity matrix.

CKI/Dco is known to have a large amount of interaction partners. A possible reason for low amount of proteins copurifed and subsequently identified in our expeiment might result from weak nature of interaction between Dco and its substrates. Phosphorylations are dynamical processes presuming transient interactions.

As the weak interactions had not probably been kept during the second purification step, the MS analysis was executed also on the samples recovered after the AcTEV protease cleavage. A high number of contaminants had been present. Therefore, data avaluation had to be performed via comparison of the positive and negative datasets followed by subtraction of negative hits. The list of proteins involved in the datasets resulted from three independent purifications. Proteins identified together with Dco and characterized with minimally three independent peptides were taken into consideration as probable substrates of Dco. Literature and database search was subsequently performed to link indicated interactors with known interaction partners. In the following text, hypothetical relationships between five selected interaction partners indicated by MS analysis and Dco are outlined in detail.

Apart from the proteins mentioned in following text, other copurified proteins should be also kept in mind, as a novel role of Dco could be revealed. There are many proteins with unknown function listed. In priciple, all of them could eventually prove to be false positives. The spectrum of common Dco substrates could be changed due to its overexpression. Or, since wild type form of *dco* gene was present in the fly genome and translated, the presence of tag could handicap the tagged-Dco in comparison with its wildtype form. Therefore, in order

to account affinity-purified proteins as a true interactors of Dco, they have to be indepently confirmed by different experimental technique, e.g. by immunoprecipitation using Dco-copurified proteins as a bait. In addition, the tandem affinity purification could be repeated more times to improve the statistical relevance.

4.1. Hook, Shibire, Heat shock protein cognate 70-4, dynein, Scribbler, A kinase anchor protein 550 and β-spectrin Copurify with Dco.

According to our results, Heat shock protein cognate 4 (Hsc70-4), Shibire (Shi), Hook (Hk), dynein heavy chain 64C and 62B, Scribbler (Sbb), A kinase anchor protein 550 (AKAP 550) and β-spectrin are possible interactors of Dco and all of them probably contain the phospohorylation site for CKI. There is a common background that connects these copurified proteins - endocytosis and molecular trafficking.

Endocytosis is a process common to all eukaryotic cells that plays a critical role not only in the internalization of extracellular macromolecules, but also in the down-regulation of signaling receptors from the cell surface. One of the most common way of endocytosis is the clathrin-mediated pathway, a selective internalization of receptors and bound ligands via clathrin-coated vesicles (CCVs), (Schmid, 1997; Kirchhausen, 2000).

In human, it has been proven that Hsc70 binds to the dynamin, *Drosophila* homologue Shi, and it is involved in early steps of CCV formation (Newmyer et al., 2003). Moreover, Hsc70 that has been implicated in many stages of this CCV cycle, may have a role in proper organization of endosomal compartments (Chang et al., 2002) and is considered to be the uncoating ATPase known to aggregate upon dissociation of the CCV coat (Drucker et al., 1996). The forming endocytic vesicles are cleaved from membranes via the function of dynamin (Hinshaw, 2000).

Since it was shown that Hk binds to organelles and to microtubules and that dynein is involved in the intracellular transport of organelles and cytoplasmic constituents as well, there is a possibility that Dco is involved in the process of CCV formation or its transport.Interestingly, cellular localization studies showed, that CKIδ localizes to the golgi and microtubule network in interphase cells, consistently with its role in trafficking (Behrend et al., 2000). CKIε has been also shown to be involved in protein trafficking and lysosome biosynthesis (Yin et al., 2006).

We have observed presence of AKAP 550 in the Dco-copurified fraction. AKAP 550 (also known as Rugose) was shown to be expressed in many cells in nearly all tissues throughout the lifespan of the fly (Han et al., 1997). AKAPs function as scaffold proteins,

providing an organizing centre, around which various protein kinases and phosphatases can be assembled to traffic signalling molecules to unique subcellular microdomains (Malbon et al., 2004).

Moreover, Holleran et al., 2001 suggested that dynein may dock to vesicular cargo via connection with an organelle-associated spectrin network (when observing dynein and spectrin co-purificants on vesicles isolated from rat brain). This could be in congruence with our observations in *Drosophila*, as dynein and β-spectrin were purified together with Dco and other components of the molecular trafficking.

Several proteins associated with CCVs have been known as substrate for protein kinases. CCVs contain CKII, and clathrin light chain β has been shown to be a good substrate for this enzyme (Bar-Zvi and Branton, 1986; Loeb et al., 1989). Association and dissociation cycle of CCV is guided by phosphorylation as well (Ghosh and Kornfeld, 2003; Maldonado-Báez and Wendland, 2006); causing in many cases conformation changes of the coat protein subunits (for review, see Langer et al., 2007). Dco may also participate in phosphorylation of CCVs.

On the other hand, a different explanation may be also possible. The Dco-copurified proteins exhibiting connections with vesicule trafficking could serve as Dco transporter between the Golgi network and lysosomes. Although results of the rescue experiment imply that the tagged protein is at least partially functional, the level of experssion would not be desirable for the larvae and degradation of the major portion of overexpressed Dco could occur.

4.2. Possible Relationship among CKIε, CdGAPr and PR2.

Our data suggest that Dco, *Drosophila melanogaster* homolog of mammalian CKIε, binds to PR2 and CdGAPr. Both of them contain predicted phosphorylation site for CKI. These two proteins are known to have common binding partner, Rac (Burbelo et al., 1995; Lamarche-Vane and Hall, 1998). During non-canonical Wingless signaling, Wnt stimulation through the Frizzled (Fz) receptor activates Dishevelled (Dsh), which then induces the activation Rac via an unknown mechanism (Habas and He, 2007); (Fig. 4.1). As Dishevelled is a confirmed phosphorylation target of Dco (Cong et al., 2004), we might speculate that Dsh together with Dco regulates Rac activity via CdGAPr and/or PR2.

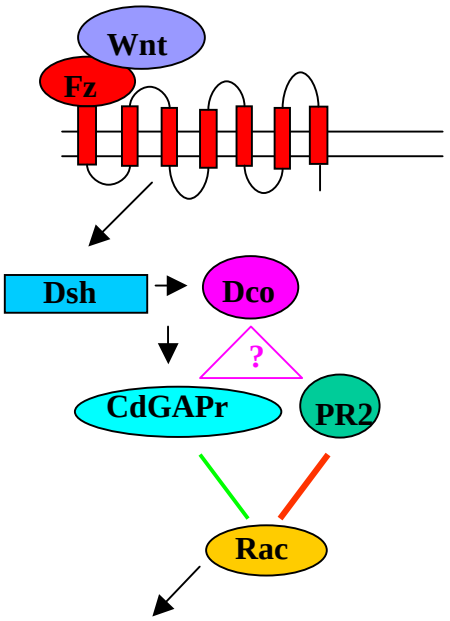

Fig. 4.1 The hypothetical relationship among Dco, CdGAPr and PR2 (marked with pink triangle) during non-canonical signaling. The scheme summarizes the interactions described in the text above. PR2 interaction with Rac known from *Drosophila* marked by a red line and regulation of Rac by mammalian homolog of *Drosophila* CdGAPr marked by a green line.

4.3. Possible Interaction between Dco and Rpn6

Rpn6, another protein copurified with Dco, is a subunit of the 26S proteasome. The ubiquitin (Ub)/26S proteasome system serves as proteolytic machinery for the degradation of a certain set of substrates (from substrate labelling by phosphorylation and ubiquitination to

complete proteolytic cleavage). There is increasing evidence that the Ub/26S proteasome system regulates the stability of important cellular proteins in cooperation with the COP9 signalosome (CSN). Huang et al., 2005 showed that CSN directly interacted with the 26S proteasome. Moreover, it was proven that *Drosophila* non-ATPase subunit of the 26S proteasome, Rpn6, physically interacted with CSN through its Alien/CSN2 subunit (Lier and Paululat, 2002).

The COP9 signalosome (CSN) complex possesses kinase activity that phosphorylates substrates such as tumor suppressor p53 (Bech-Otschir et al., 2001). Alterations in its phosphorylation status can abolish its function resulting in uncontrolled growth of cells. p53 phosphorylation dedicates the protein to rapid degradation by the ubiquitin-26S proteasome system. Further, it has been shown that Dco human homologue CK1ε phosphorylate p53 *in vitro* and in cultured cells (Knippschild et al., 1997).

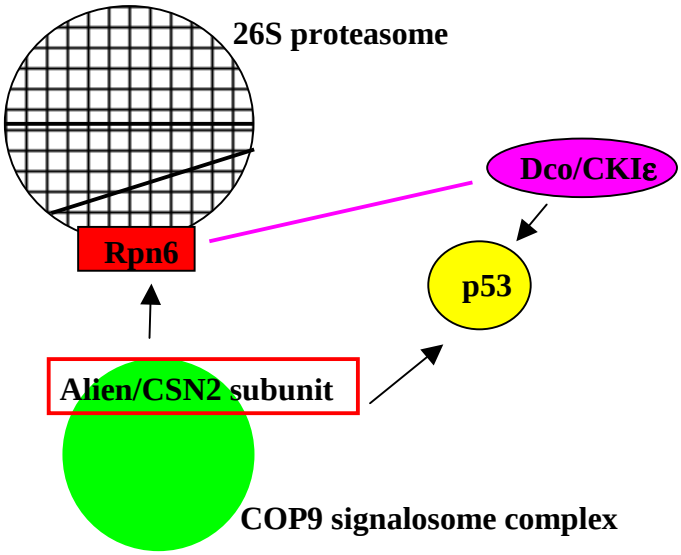

Fig. 4.2: Possible relationship among Dco/CKIε, Rpn6 subunit of 26S proteasome and COP9 signalosome complex. Interaction revealed by our experiments represented by pink line. The scheme summarizes the interactions described in the text above.

These data along with the fact that Rpn6 copurifies with Dco in our experiments, suggest that Rpn6 might contribute with its kinase activity to selective p53 phosphorylation and degradation through a hypothetical Ub/26S proteasome/CSN system (Fig. 4.2).

4.4. Possible Interaction among Dco, Scribbler and β-spectrin

Our results suggest that Dco interacts with Scribbler (also known as Brakeless) and β-spectrin and both of them contain predicted phosphorylation site for CKI. Genetic interaction betwen *scribbler (sbb)* and *merlin* was previously proven. *Sbb* modifies both loss-of-function and dominant-negative *merlin* phenotypes (LaJeunesse et al., 2001). Using the yeast two-hybrid method Merlin human homologue NF2 was proven to interact with β-spectrin (Scoles et al., 1998).

Merlin mutants revealed obvious overgrowth phenotype of the imaginal discs. Mutations in *merlin* dominantly enhanced phenotypes of mutations in another gene *expanded* (McCartney et al., 2000). Interestingly, the phenotype of overgrown discs of *expanded* homozygotes is similar in appearance to the discs of *dco3* mutant (Boedigheimer and Laughon, 1993).

Taken into consideration that *merlin* and *dco* mutant overgrowth phenotype of the imaginal discs in *Drosophila* are highly similar and both of them possibly integrate with β-spectrin and Scribbler, further investigation of their hypothetical relationship would be of particular interest.

Dco, Merlin and Expanded have been shown to be components of the Fat/Hippo pathway (Fig. 4.3). Hippo pathway has been proven to be the general mediator of Fat signaling in growth control. Hippo pathway limits organ size by inhibiting cell proliferation and promoting apoptosis. Fly cells with mutant components of this pathway are able to proliferate at the expense of their normal, neighbouring cells through supercompetition (wildtype cells are eliminated from mosaic tissues that contain cells with mutations). Moreover in mammals, loss of Hippo signaling enables cells to acquire tumorigenic capabilities. Further, alterations in human homologue of *Drosophila merlin*, the *NF2* gene, cause all tumours that occur in patients suffering from neurofibromatosis type 2, all spontaneous schwannomas and the majority of meningiomas (for review see, Hanneman, 2008).

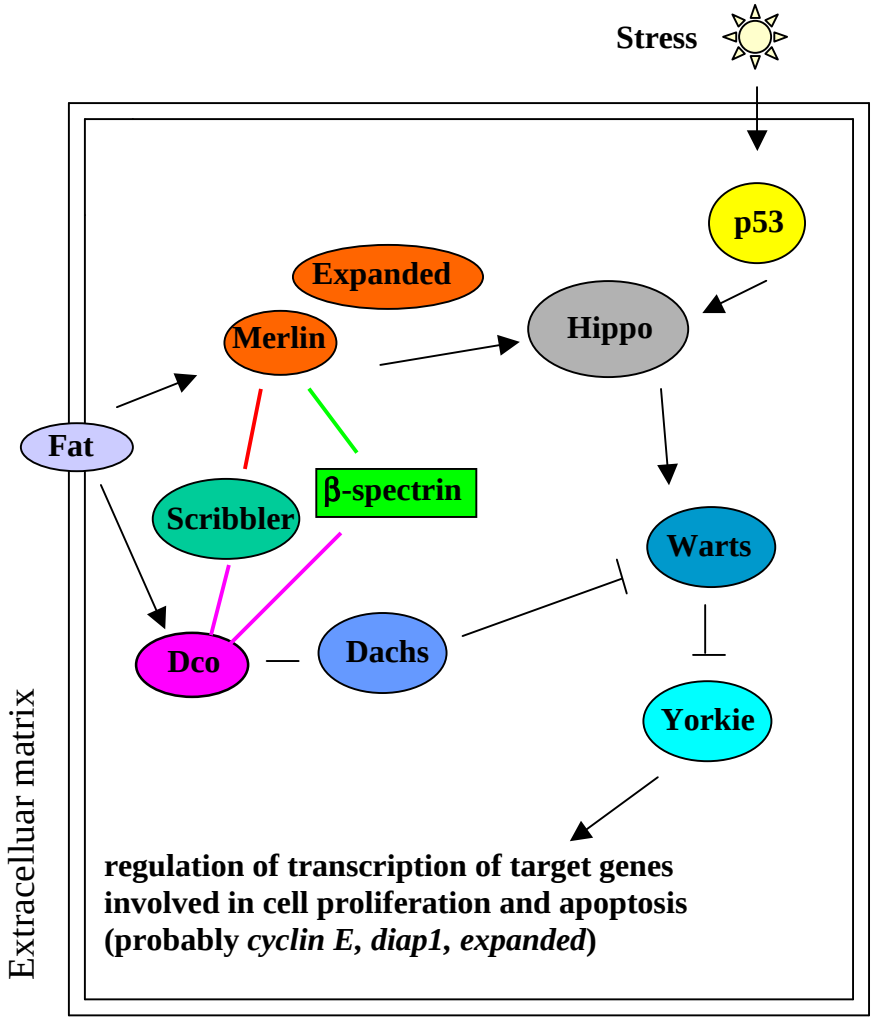

Fig. 4.3: Simplified scheme of regulation of Hippo signalling according to Cho et al., 2006; Saucedo and Edgar, 2007 and Hanemann, 2008. Dco is positioned upstream of Dachs, and both of them together with Fat influence the protein level of Warts. Merlin, Expanded and Hippo also exhibit the Fat pathway phenotypes, but regulate Warts activity independently. Fat functions primarily through Expanded, probably mediated through Merlin to fully induce Hippo signalling. They induce phosphorylation of Warts, and overexpression of Expanded alone leads to phosphorylation of Hippo (Hamaratoglu et al., 2006). Activated Warts phosphorylates and inactivates the transcriptional co-activator Yorkie. Although the transcription factors that Yorkie modulates are unknown in flies, several genes have been demonstrated to be induced following activation of Yorkie. These include the G1–S regulator *cyclin E*, the *drosophila inhibitor of apoptosis-1 (diap1)* and *expanded*, an upstream component of Hippo signalling. Moreover, upon celluar stress, p53 seems to promote Hippo activity by phosphorylation thereby sensitizing cells to apoptosis through repression of *diap1*; (Colombani et al., 2006). Scribbler and β-spectrin were revealed as Dco interactors by our experiments (represented by pink lines). Merlin interaction with Scribbler marked by a red line and the relationship between its human homologue NF2 with β-spectrin by a green line.

Interesting hypothesis comes up with the possibility, that Scribbler alters Merlin subcellular localization in epithelial and neuronal tissues via regulating Merlin trafficking (LaJeunesse et al., 2001). Moreover, Merlin together with Expanded have been shown to associate with endocytotic vesicles (McCartney et al., 2000; Maitra et al., 2006). It has been proposed that Merlin and Expanded limit the levels of receptors (Notch, Wingless and EGFR signaling) at the plasma membrane by promoting endocytosis. Saucedo and Edgar, 2007 imply that Fat could promote the endocytosis of receptors by Expanded and Merlin, therefore coordinating multiple growth-regulating pathways. Thus, the supposed hyphothetical connection between Dco and endocytosis (described earlier) could eventually serve as a tool for the Fat signaling.

4.5. Mushroom body defect protein (Mud)

Finally, we have observed another Dco-copurificant, the Mushroom body defect protein (Mud). It has been proven that Mud localizes to centrosomes during mitosis to regulate centrosomal organization (Izumi et al., 2006). Mutants of Mud disrupt mitotic spindle orientation in neuroblasts, and also can also exhibit overproliferation, although this effect is weak (Bowman et al., 2006). Mammalian CKIε is enriched at the centrosomes in interphase cells and at the spindle during mitosis. It was shown to be localized at the centrosome, probably through association with centrosomal scaffold protein AKAP450 (Sillibourne et al., 2002). According to our experiments and previously known facts, there could be a connection among Dco, Mud and centrosome organisation.

5. Conclusions

The construct containing the coding region of *dco*, *Drosophila* homologue of human CKIε, was fused with the TAP tag into the pUAST vector. Using this vectror, *Drosophila* transgenic lines were generated and the tagged Dco protein was expressed in imaginal discs of late third instar larvae using UAS/Gal4 system. TAP-tagged Dco was purified from crude Drosophila larvae extracts under native conditions using tandem affinity purification (TAP). Proteins copurified with the Dco were identified using MS analysis. Complete, two-step TAP procedure resulted in identification of two posible interactors of Dco, heat shock protein cognate 70-4 and β-spectrin. One-step affinity purification followed by MS analysis indicated, apart from heat shock protein cognate 70-4 and β-spectrin, 33 other possible interaction partners of Dco. Although, there are justified functional relationships between Dco and the indicated proteins, these proteins need to be independently verified as true interaction partners.

6. References

Bae, K., and Edery, I. (2006). Regulating a circadian clock's period, phase and amplitude by phosphorylation: insights from Drosophila. J Biochem *140*, 609-617.

Bar-Zvi, D., and Branton, D. (1986). Clathrin-coated vesicles contain two protein kinase activities. Phosphorylation of clathrin beta-light chain by casein kinase II. J Biol Chem *261*, 9614-9621.

Behrend, L., Stoter, M., Kurth, M., Rutter, G., Heukeshoven, J., Deppert, W., and Knippschild, U. (2000). Interaction of casein kinase 1 delta (CK1delta) with post-Golgi structures, microtubules and the spindle apparatus. Eur J Cell Biol *79*, 240-251.

Bech-Otschir, D., Kraft, R., Huang, X., Henklein, P., Kapelari, B., Pollmann, C., and Dubiel, W. (2001). COP9 signalosome-specific phosphorylation targets p53 to degradation by the ubiquitin system. EMBO J *20*, 1630-1639.

Blom, N., Sicheritz-Ponten, T., Gupta, R., Gammeltoft, S., and Brunak, S. (2004). Prediction of post-translational glycosylation and phosphorylation of proteins from the amino acid sequence. Proteomics *4*, 1633-1649.

Boedigheimer, M., and Laughon, A. (1993). Expanded: a gene involved in the control of cell proliferation in imaginal discs. Development *118*, 1291-1301.

Boivin, P. (1988). Role of the phosphorylation of red blood cell membrane proteins. Biochem J *256*, 689-695.

Bowman, S.K., Neumuller, R.A., Novatchkova, M., Du, Q., and Knoblich, J.A. (2006). The Drosophila NuMA Homolog Mud regulates spindle orientation in asymmetric cell division. Dev Cell *10*, 731-742.

Burbelo, P.D., Drechsel, D., and Hall, A. (1995). A conserved binding motif defines numerous candidate target proteins for both Cdc42 and Rac GTPases. J Biol Chem *270*, 29071-29074.

Burckstummer, T., Bennett, K.L., Preradovic, A., Schutze, G., Hantschel, O., Superti-Furga, G., and Bauch, A. (2006). An efficient tandem affinity purification procedure for interaction proteomics in mammalian cells. Nat Methods *3*, 1013-1019.

Colombani, J., Polesello, C., Josue, F., and Tapon, N. (2006). Dmp53 activates the Hippo pathway to promote cell death in response to DNA damage. Curr Biol *16*, 1453-1458.

Cong, F., Schweizer, L., and Varmus, H. (2004). Casein kinase Iepsilon modulates the signaling specificities of dishevelled. Mol Cell Biol *24*, 2000-2011.

Cyran, S.A., Yiannoulos, G., Buchsbaum, A.M., Saez, L., Young, M.W., and Blau, J. (2005). The double-time protein kinase regulates the subcellular localization of the Drosophila clock protein period. J Neurosci *25*, 5430-5437.

Dahmann, Ch. (2008). Drosophila Methods and Protocols. Humana Press, Totowa, USA, 437 pp.

Drucker, M., Happel, N., and Robinson, D.G. (1996). Localization and properties of kinases in clathrin-coated vesicles from zucchini hypocotyls. Eur J Biochem *240*, 570-575.

Duffy, J.B. (2002). GAL4 system in Drosophila: a fly geneticist's Swiss army knife. Genesis *34*, 1-15.

Dumaz, N., Milne, D.M., and Meek, D.W. (1999). Protein kinase CK1 is a p53-threonine 18 kinase which requires prior phosphorylation of serine 15. FEBS Lett *463*, 312-316.

Ebisawa, T., Uchiyama, M., Kajimura, N., Mishima, K., Kamei, Y., Katoh, M., Watanabe, T., Sekimoto, M., Shibui, K., Kim, K., *et al.* (2001). Association of structural polymorphisms in the human period3 gene with delayed sleep phase syndrome. EMBO Rep *2*, 342-346.

Emery, J., Lucassen, A., and Murphy, M. (2001). Common hereditary cancers and implications for primary care. Lancet *358*, 56-63.

Ferlay, J., Autier, P., Boniol, M., Heanue, M., Colombet, M., and Boyle, P. (2007). Estimates of the cancer incidence and mortality in Europe in 2006. Ann Oncol *18*, 581-592.

Ferrarese, A., Marin, O., Bustos, V.H., Venerando, A., Antonelli, M., Allende, J.E., and Pinna, L.A. (2007). Chemical dissection of the APC Repeat 3 multistep phosphorylation by the concerted action of protein kinases CK1 and GSK3. Biochemistry *46*, 11902-11910.

Fischer, J.A., Giniger, E., Maniatis, T., and Ptashne, M. (1988). GAL4 activates transcription in Drosophila. Nature *332*, 853-856.

Flajolet, M., He, G., Heiman, M., Lin, A., Nairn, A.C., and Greengard, P. (2007). Regulation of Alzheimer's disease amyloid-beta formation by casein kinase I. Proc Natl Acad Sci U S A *104*, 4159-4164.

Fuja, T.J., Lin, F., Osann, K.E., and Bryant, P.J. (2004). Somatic mutations and altered expression of the candidate tumor suppressors CSNK1 epsilon, DLG1, and EDD/hHYD in mammary ductal carcinoma. Cancer Res *64*, 942-951.

Gavin, A.C., Aloy, P., Grandi, P., Krause, R., Boesche, M., Marzioch, M., Rau, C., Jensen, L.J., Bastuck, S., Dumpelfeld, B., *et al.* (2006). Proteome survey reveals modularity of the yeast cell machinery. Nature *440*, 631-636.

Ghosh, P., and Kornfeld, S. (2003). AP-1 binding to sorting signals and release from clathrin-coated vesicles is regulated by phosphorylation. J Cell Biol *160*, 699-708.

Ghoshal, N., Smiley, J.F., DeMaggio, A.J., Hoekstra, M.F., Cochran, E.J., Binder, L.I., and Kuret, J. (1999). A new molecular link between the fibrillar and granulovacuolar lesions of Alzheimer's disease. Am J Pathol *155*, 1163-1172.

Gietzen, K.F., and Virshup, D.M. (1999). Identification of inhibitory autophosphorylation sites in casein kinase I epsilon. J Biol Chem *274*, 32063-32070.

Griffiths, A.J.F., Gelbart, W.M., Miller, J.H., Lewontin, R.C. (1999). Modern Genetic Analysis. W H Freeman & Co, New York, USA, 675pp.

Gross, S.D., and Anderson, R.A. (1998). Casein kinase I: spatial organization and positioning of a multifunctional protein kinase family. Cell Signal *10*, 699-711.

Ha, N.C., Tonozuka, T., Stamos, J.L., Choi, H.J., and Weis, W.I. (2004). Mechanism of phosphorylation-dependent binding of APC to beta-catenin and its role in beta-catenin degradation. Mol Cell *15*, 511-521.

Habas, R., and He, X. (2007). Cell signaling: moving to a Wnt-Rap. Curr Biol *17*, R474-477.

Hamaratoglu, F., Willecke, M., Kango-Singh, M., Nolo, R., Hyun, E., Tao, C., Jafar-Nejad, H., and Halder, G. (2006). The tumour-suppressor genes NF2/Merlin and Expanded act through Hippo signalling to regulate cell proliferation and apoptosis. Nat Cell Biol *8*, 27-36.

Han, J.D., Baker, N.E., and Rubin, C.S. (1997). Molecular characterization of a novel A kinase anchor protein from Drosophila melanogaster. J Biol Chem *272*, 26611-26619.

Hanemann, C.O. (2008). Magic but treatable? Tumours due to loss of merlin. Brain *131*, 606-615.

Hardin, P.E. (2005). The circadian timekeeping system of Drosophila. Curr Biol *15*, R714-722.

Hinshaw, J.E. (2000). Dynamin and its role in membrane fission. Annu Rev Cell Dev Biol *16*, 483-519.

Holleran, E.A., Ligon, L.A., Tokito, M., Stankewich, M.C., Morrow, J.S., and Holzbaur, E.L. (2001). beta III spectrin binds to the Arp1 subunit of dynactin. J Biol Chem *276*, 36598-36605.

Huang, X., Hetfeld, B.K., Seifert, U., Kahne, T., Kloetzel, P.M., Naumann, M., Bech-Otschir, D., and Dubiel, W. (2005). Consequences of COP9 signalosome and 26S proteasome interaction. FEBS J *272*, 3909-3917.

Chang, H.C., Newmyer, S.L., Hull, M.J., Ebersold, M., Schmid, S.L., and Mellman, I. (2002). Hsc70 is required for endocytosis and clathrin function in Drosophila. J Cell Biol *159*, 477-487.

Cho, E., Feng, Y., Rauskolb, C., Maitra, S., Fehon, R., and Irvine, K.D. (2006). Delineation of a Fat tumor suppressor pathway. Nat Genet *38*, 1142-1150.

Izumi, Y., Ohta, N., Hisata, K., Raabe, T., and Matsuzaki, F. (2006). Drosophila Pins-binding protein Mud regulates spindle-polarity coupling and centrosome organization. Nat Cell Biol *8*, 586-593.

Jia, J., Zhang, L., Zhang, Q., Tong, C., Wang, B., Hou, F., Amanai, K., and Jiang, J. (2005). Phosphorylation by double-time/CKIepsilon and CKIalpha targets cubitus interruptus for Slimb/beta-TRCP-mediated proteolytic processing. Dev Cell *9*, 819-830.

Jursnich, V.A., Fraser, S.E., Held, L.I., Jr., Ryerse, J., and Bryant, P.J. (1990). Defective gap-junctional communication associated with imaginal disc overgrowth and degeneration caused by mutations of the dco gene in Drosophila. Dev Biol *140*, 413-429.

Kannanayakal, T.J., Tao, H., Vandre, D.D., and Kuret, J. (2006). Casein kinase-1 isoforms differentially associate with neurofibrillary and granulovacuolar degeneration lesions. Acta Neuropathol *111*, 413-421.

Kawakami, F., Suzuki, K., and Ohtsuki, K. (2008). A novel consensus phosphorylation motif in sulfatide- and cholesterol-3-sulfate-binding protein substrates for CK1 in vitro. Biol Pharm Bull *31*, 193-200.

Kim, E.Y., and Edery, I. (2006). Balance between DBT/CKIepsilon kinase and protein phosphatase activities regulate phosphorylation and stability of Drosophila CLOCK protein. Proc Natl Acad Sci U S A *103*, 6178-6183.

Kirchhausen, T. (2000). Three ways to make a vesicle. Nat Rev Mol Cell Biol *1*, 187-198.

Kivimae, S., Saez, L., and Young, M.W. (2008). Activating PER repressor through a DBT-directed phosphorylation switch. PLoS Biol *6*, e183.

Klein, T.J., Jenny, A., Djiane, A., and Mlodzik, M. (2006). CKIepsilon/discs overgrown promotes both Wnt-Fz/beta-catenin and Fz/PCP signaling in Drosophila. Curr Biol *16*, 1337-1343.

Kloss, B., Price, J.L., Saez, L., Blau, J., Rothenfluh, A., Wesley, C.S., and Young, M.W. (1998). The Drosophila clock gene double-time encodes a protein closely related to human casein kinase Iepsilon. Cell *94*, 97-107.

Knippschild, U., Gocht, A., Wolff, S., Huber, N., Lohler, J., and Stoter, M. (2005a). The casein kinase 1 family: participation in multiple cellular processes in eukaryotes. Cell Signal *17*, 675-689.

Knippschild, U., Milne, D.M., Campbell, L.E., DeMaggio, A.J., Christenson, E., Hoekstra, M.F., and Meek, D.W. (1997). p53 is phosphorylated in vitro and in vivo by the delta and epsilon isoforms of casein kinase 1 and enhances the level of casein kinase 1 delta in response to topoisomerase-directed drugs. Oncogene *15*, 1727-1736.

Knippschild, U., Wolff, S., Giamas, G., Brockschmidt, C., Wittau, M., Wurl, P.U., Eismann, T., and Stoter, M. (2005b). The role of the casein kinase 1 (CK1) family in different signaling pathways linked to cancer development. Onkologie *28*, 508-514.

LaJeunesse, D.R., McCartney, B.M., and Fehon, R.G. (2001). A systematic screen for dominant second-site modifiers of Merlin/NF2 phenotypes reveals an interaction with blistered/DSRF and scribbler. Genetics *158*, 667-679.

Lamarche-Vane, N., and Hall, A. (1998). CdGAP, a novel proline-rich GTPase-activating protein for Cdc42 and Rac. J Biol Chem *273*, 29172-29177.

Langer, J.D., Stoops, E.H., Bethune, J., and Wieland, F.T. (2007). Conformational changes of coat proteins during vesicle formation. FEBS Lett *581*, 2083-2088.

Lier, S., and Paululat, A. (2002). The proteasome regulatory particle subunit Rpn6 is required for Drosophila development and interacts physically with signalosome subunit Alien/CSN2. Gene *298*, 109-119.

Lindsley, D.L., Zimm, G.G. (1992). The Genome of Drosophila melanogaster. Academic Press, Inc. San Diego, California, USA, viii + 1133pp.

Loeb, J.E., Cantournet, B., Vartanian, J.P., Goris, J., and Merlevede, W. (1989). Phosphorylation/dephosphorylation of the beta light chain of clathrin from rat liver coated vesicles. Eur J Biochem *182*, 195-202.

Lowrey, P.L., Shimomura, K., Antoch, M.P., Yamazaki, S., Zemenides, P.D., Ralph, M.R., Menaker, M., and Takahashi, J.S. (2000). Positional syntenic cloning and functional characterization of the mammalian circadian mutation tau. Science *288*, 483-492.

Maitra, S., Kulikauskas, R.M., Gavilan, H., and Fehon, R.G. (2006). The tumor suppressors Merlin and Expanded function cooperatively to modulate receptor endocytosis and signaling. Curr Biol *16*, 702-709.

Malbon, C.C., Tao, J., and Wang, H.Y. (2004). AKAPs (A-kinase anchoring proteins) and molecules that compose their G-protein-coupled receptor signalling complexes. Biochem J *379*, 1-9.

Maldonado-Baez, L., and Wendland, B. (2006). Endocytic adaptors: recruiters, coordinators and regulators. Trends Cell Biol *16*, 505-513.

Manno, S., Takakuwa, Y., Nagao, K., and Mohandas, N. (1995). Modulation of erythrocyte membrane mechanical function by beta-spectrin phosphorylation and dephosphorylation. J Biol Chem *270*, 5659-5665.

Marin, O., Burzio, V., Boschetti, M., Meggio, F., Allende, C.C., Allende, J.E., and Pinna, L.A. (2002). Structural features underlying the multisite phosphorylation of the A domain of the NF-AT4 transcription factor by protein kinase CK1. Biochemistry *41*, 618-627.

Marin, O., Bustos, V.H., Cesaro, L., Meggio, F., Pagano, M.A., Antonelli, M., Allende, C.C., Pinna, L.A., and Allende, J.E. (2003). A noncanonical sequence phosphorylated by casein kinase 1 in beta-catenin may play a role in casein kinase 1 targeting of important signaling proteins. Proc Natl Acad Sci U S A *100*, 10193-10200.

McCartney, B.M., Kulikauskas, R.M., LaJeunesse, D.R., and Fehon, R.G. (2000). The neurofibromatosis-2 homologue, Merlin, and the tumor suppressor expanded function together in Drosophila to regulate cell proliferation and differentiation. Development *127*, 1315-1324.

McPherson, K., Steel, C.M., and Dixon, J.M. (2000). ABC of breast diseases. Breast cancer-epidemiology, risk factors, and genetics. BMJ *321*, 624-628.

Modak, C., and Bryant, P. (2008). Casein Kinase I epsilon positively regulates the Akt pathway in breast cancer cell lines. Biochem Biophys Res Commun *368*, 801-807.

Muskus, M.J., Preuss, F., Fan, J.Y., Bjes, E.S., and Price, J.L. (2007). Drosophila DBT lacking protein kinase activity produces long-period and arrhythmic circadian behavioral and molecular rhythms. Mol Cell Biol *27*, 8049-8064.

Newmyer, S.L., Christensen, A., and Sever, S. (2003). Auxilin-dynamin interactions link the uncoating ATPase chaperone machinery with vesicle formation. Dev Cell *4*, 929-940.

Okamura, H., Garcia-Rodriguez, C., Martinson, H., Qin, J., Virshup, D.M., and Rao, A. (2004). A conserved docking motif for CK1 binding controls the nuclear localization of NFAT1. Mol Cell Biol *24*, 4184-4195.

Okano, M., Yokoyama, T., Miyanaga, T., and Ohtsuki, K. (2004). Activation of C-kinase eta through its cholesterol-3-sulfate-dependent phosphorylation by casein kinase I in vitro. Biol Pharm Bull *27*, 109-112.

Polakis, P. (2007). The many ways of Wnt in cancer. Curr Opin Genet Dev *17*, 45-51.

Potter, C.J., Turenchalk, G.S., and Xu, T. (2000). Drosophila in cancer research. An expanding role. Trends Genet *16*, 33-39.

Price, M.A. (2006). CKI, there's more than one: casein kinase I family members in Wnt and Hedgehog signaling. Genes Dev *20*, 399-410.

Puig, O., Caspary, F., Rigaut, G., Rutz, B., Bouveret, E., Bragado-Nilsson, E., Wilm, M., and Seraphin, B. (2001). The tandem affinity purification (TAP) method: a general procedure of protein complex purification. Methods *24*, 218-229.

Pulgar, V., Marin, O., Meggio, F., Allende, C.C., Allende, J.E., and Pinna, L.A. (1999). Optimal sequences for non-phosphate-directed phosphorylation by protein kinase CK1 (casein kinase-1)--a re-evaluation. Eur J Biochem *260*, 520-526.

Rivers, A., Gietzen, K.F., Vielhaber, E., and Virshup, D.M. (1998). Regulation of casein kinase I epsilon and casein kinase I delta by an in vivo futile phosphorylation cycle. J Biol Chem *273*, 15980-15984.

Sakaguchi, K., Saito, S., Higashimoto, Y., Roy, S., Anderson, C.W., and Appella, E. (2000). Damage-mediated phosphorylation of human p53 threonine 18 through a cascade mediated by a casein 1-like kinase. Effect on Mdm2 binding. J Biol Chem *275*, 9278-9283.

Saucedo, L.J., and Edgar, B.A. (2007). Filling out the Hippo pathway. Nat Rev Mol Cell Biol *8*, 613-621.

Scoles, D.R., Huynh, D.P., Morcos, P.A., Coulsell, E.R., Robinson, N.G., Tamanoi, F., and Pulst, S.M. (1998). Neurofibromatosis 2 tumour suppressor schwannomin interacts with betaII-spectrin. Nat Genet *18*, 354-359.

Schmid, S.L. (1997). Clathrin-coated vesicle formation and protein sorting: an integrated process. Annu Rev Biochem *66*, 511-548.

Sillibourne, J.E., Milne, D.M., Takahashi, M., Ono, Y., and Meek, D.W. (2002). Centrosomal anchoring of the protein kinase CK1delta mediated by attachment to the large, coiled-coil scaffolding protein CG-NAP/AKAP450. J Mol Biol *322*, 785-797.

Songyang, Z., Lu, K.P., Kwon, Y.T., Tsai, L.H., Filhol, O., Cochet, C., Brickey, D.A., Soderling, T.R., Bartleson, C., Graves, D.J., *et al.* (1996). A structural basis for substrate specificities of protein Ser/Thr kinases: primary sequence preference of casein kinases I and II, NIMA, phosphorylase kinase, calmodulin-dependent kinase II, CDK5, and Erk1. Mol Cell Biol *16*, 6486-6493.

Sotgia, F., Williams, T.M., Cohen, A.W., Minetti, C., Pestell, R.G., and Lisanti, M.P. (2005). Caveolin-1-deficient mice have an increased mammary stem cell population with upregulation of Wnt/beta-catenin signaling. Cell Cycle *4*, 1808-1816.

Strutt, H., Price, M.A., and Strutt, D. (2006). Planar polarity is positively regulated by casein kinase Iepsilon in Drosophila. Curr Biol *16*, 1329-1336.

Takano, A., Uchiyama, M., Kajimura, N., Mishima, K., Inoue, Y., Kamei, Y., Kitajima, T., Shibui, K., Katoh, M., Watanabe, T., *et al.* (2004). A missense variation in human casein kinase I epsilon gene that induces functional alteration and shows an inverse association with circadian rhythm sleep disorders. Neuropsychopharmacology *29*, 1901-1909.

Umar, S., Wang, Y., Morris, A.P., and Sellin, J.H. (2007). Dual alterations in casein kinase I-epsilon and GSK-3beta modulate beta-catenin stability in hyperproliferating colonic epithelia. Am J Physiol Gastrointest Liver Physiol *292*, G599-607.

Veraksa, A., Bauer, A., and Artavanis-Tsakonas, S. (2005). Analyzing protein complexes in Drosophila with tandem affinity purification-mass spectrometry. Dev Dyn *232*, 827-834.

Vielhaber, E., and Virshup, D.M. (2001). Casein kinase I: from obscurity to center stage. IUBMB Life *51*, 73-78.

Xu, Y., Padiath, Q.S., Shapiro, R.E., Jones, C.R., Wu, S.C., Saigoh, N., Saigoh, K., Ptacek, L.J., and Fu, Y.H. (2005). Functional consequences of a CKIdelta mutation causing familial advanced sleep phase syndrome. Nature *434*, 640-644.

Yang, W.S., and Stockwell, B.R. (2008). Inhibition of casein kinase 1-epsilon induces cancer-cell-selective, PERIOD2-dependent growth arrest. Genome Biol *9*, R92.

Yin, H., Laguna, K.A., Li, G., and Kuret, J. (2006). Dysbindin structural homologue CK1BP is an isoform-selective binding partner of human casein kinase-1. Biochemistry *45*, 5297-5308.

Zhang, L., Jia, J., Wang, B., Amanai, K., Wharton, K.A., Jr., and Jiang, J. (2006). Regulation of wingless signaling by the CKI family in Drosophila limb development. Dev Biol *299*, 221-237.

Zhao, B., Lei, Q.Y., and Guan, K.L. (2008). The Hippo-YAP pathway: new connections between regulation of organ size and cancer. Curr Opin Cell Biol *20*, 638-646.

Zilian, O., Frei, E., Burke, R., Brentrup, D., Gutjahr, T., Bryant, P.J., and Noll, M. (1999). double-time is identical to discs overgrown, which is required for cell survival, proliferation and growth arrest in Drosophila imaginal discs. Development *126*, 5409-5420.

7. Appendix

Tab. A1: Tandem affinity purified proteins of *D. melanogaster*, identified by the PLGS 2.3 software by MS^E Identity method.

Entry – gene code according to Flybase.org, Peptides – the number of identified peptides, Theoretical peptides – the number of computed tryptic peptides resulting from the complete protein tryptic digestion, Coverage – the ratio of identified peptides to theoretical peptides. Precursor RMS Mass Error – Root Main Square Mass error of precursors (peptides) in ppm (Parts per Million). Products RMS Mass Error - Root Main Square Mass error of products (fragments) in ppm, Products RMS RT Error (min) – Root Main Square Retention Time Error - The software assigns fragment spectra to precursor spectra by their matching Retention Time; this number stands for the time difference between fragment spectra (MS^E) and precursor mass spectra (MS) in minutes.

Entry	mW (Da)	Peptides	Theoretical Peptides	Coverage (%)	Precursor RMS Mass Error (ppm)	Products RMS Mass Error (ppm)	Products RMS RT Error (min)
CG4264	71087	12	50	22.1198	6.2526	15.266	0.0224
CG5870	270895	7	227	2.3869	3.5096	9.4097	0.0227
CG2048	48043	3	30	7.9545	2.3194	8.5734	0.0186

Tab. A2: Dco-copurified proteins of *D. melanogaster* using the IgG matrix identified by the PLGS 2.3 software (describing data of the MS^E Identity method).

Entry – gene code according to Flybase.org, Peptides – the number of identified peptides, Theoretical peptides – the number of computed tryptic peptides resulting from the complete protein tryptic digestion, Coverage – the ratio of identified peptides to theoretical peptides. Precursor RMS Mass Error – Root Main Square Mass error of precursors (peptides) in ppm (Parts per Million). Products RMS Mass Error - Root Main Square Mass error of products (fragments) in ppm, Products RMS RT Error (min) – Root Main Square Retention Time Error - The software assigns fragment spectra to precursor spectra by their matching Retention Time; this number stands for the time difference between fragment spectra (MS^E) and precursor mass spectra (MS) in minutes.

Entry	mW (Da)	Peptides	Theoretical Peptides	Coverage (%)	Precursor RMS Mass Error (ppm)	Products RMS Mass Error (ppm)	Products RMS RT Error (min)
CG14438	371140	12	246	4.256	7.2392	14.6059	0.0267
CG7507	388246	9	289	3.0401	6.368	14.7628	0.0207
CG5794	416545	9	286	2.1604	6.2136	14.3478	0.025
CG12781	149807	8	107	6.0674	5.27	13.5382	0.022
CG3524	265700	5	171	3.3624	5.79	10.062	0.0247
CG1024	62876	5	44	10.3131	5.5214	13.0302	0.0301
CG6775	396248	4	232	1.3114	5.4745	12.4001	0.0166
CG10538	204089	4	141	2.0619	3.0048	14.1155	0.0301
CG10123	136052	4	106	3.92	3.0556	12.0906	0.0202
CG10149	47233	3	41	7.346	2.672	9.5298	0.0233
CG6985	56282	3	47	8.7824	2.9421	10.0284	0.0223
CG5580	88839	3	36	3.8751	3.9034	12.3832	0.0261
CG14438	371140	4	246	1.5696	6.4063	12.1945	0.032
CG9802	143433	5	137	6.2551	4.9968	11.4368	0.0262

Tab. A2: Continued.

Entry	mW (Da)	Peptides	Theoretical Peptides	Coverage (%)	Precursor RMS Mass Error (ppm)	Products RMS Mass Error (ppm)	Products RMS RT Error (min)
CG17282	32947	4	25	13.6364	3.5758	7.4956	0.0284
CG14967	259455	8	202	3.4771	4.5053	13.7454	0.0237
CG12233	40818	3	30	7.6923	3.9464	8.7886	0.0287
CG8193	79234	6	52	9.3567	5.3398	11.862	0.0216
CG15804	444453	5	301	2.6112	5.1569	12.7075	0.0273
CG34356	117483	5	62	4.8226	3.7281	12.9197	0.0285
CG18140	52296	4	32	13.7555	2.0168	12.0728	0.0233
CG12047	286396	3	244	1.6393	4.1088	10.531	0.0286
CG3969	84712	3	58	6.0131	4.2421	12.9916	0.0229
CG4290	149812	3	77	2.5036	3.3331	10.914	0.025
CG10653	76616	3	66	5.0074	4.4087	13.0988	0.0267
CG18102	93288	6	88	5.6627	2.936	12.2812	0.0251
CG4140	26688	3	19	12.7119	4.169	10.527	0.0275
CG7156	77024	6	55	10.7195	5.1704	13.4804	0.0179
CG7943	37339	5	33	13.5542	5.7663	15.9689	0.0254
CG34417	96967	90	75	84.3387	48.7281	56.2538	0.0276
CG1677	108948	3	170	5.9	4.6311	12.1326	0.0241

Tab. A3: Dco-copurified proteins of *D. melanogaster* using the IgG matrix identified by the PLGS 2.3 software and found by MS Survey method only. Entry – gene code according to Flybase.org, Peptides – the number of identified peptides, Coverage – the ratio of identified peptides to theoretical peptides. RMS Error – Root Main Square error.

Entry	mW (Da)	Peptides	Coverage (%)	Mean Error	RMS Error
CG13618	28827	4	10.3175	44.6198	50.0526
CG3193	84208	3	2.4217	30.737	41.1425